Preprints (www.preprints.org) | NOT PEER-REVIEWED | Posted: 4 July 2022 doi:10.20944/preprints202207.0038.v1

Article

Progeria and Aging - Omics Based Comparative Analysis

Aylin Caliskan [1], Samantha A. W. Crouch [1], Sara Giddins [1], Thomas Dandekar [1,*] and Seema Dangwal [2,*]

[1] Department of Bioinformatics, Biocenter, University of Würzburg, Würzburg, Germany; A.C. aylin.caliskan@uni-wuerzburg.de, S.A.W.C. samantha.crouch@stud-mail.uni-wuerzburg.de, S.G. sara.giddins@stud-mail.uni-wuerzburg.de, T.D. dandekar@biozentrum.uni-wuerzburg.de

[2] Stanford Cardiovascular Institute, Department of Medicine, Stanford University School of Medicine, CA, United States of America; sdangwal@stanford.edu

* Correspondence: S.D. sdangwal@stanford.edu, T.D. dandekar@biozentrum.uni-wuerzburg.de

Abstract: Since ancient times aging has also been regarded as a disease, and humankind has always strived to extend the natural lifespan. Analyzing the genes involved in aging and disease allows for finding important indicators and biological markers for pathologies and possible therapeutic targets. An example of the use of omics technologies is the research regarding aging and the rare and fatal premature aging syndrome progeria (Hutchinson-Gilford progeria syndrome, HGPS). In our study, we focused on the *in silico* analysis of differentially expressed genes (DEGs) in progeria and aging, using a publicly available RNA Seq dataset (GEO dataset GSE113957) and a variety of bioinformatics tools. We identified several genes that appear to be involved both in natural aging and progeria (KRT8, KRT18, ACKR4, CCL2, UCP2, ADAMTS15, ACTN4P1, WNT16, IGFBP2). Further analyzing these genes and the pathways involved confirmed their possible roles in aging, suggesting the need for further *in vitro* and *in vivo* research. The graphical abstract illustrates the analysis workflow we used and will introduce in the following as an example to demonstrate the power of omics and bioinformatics.

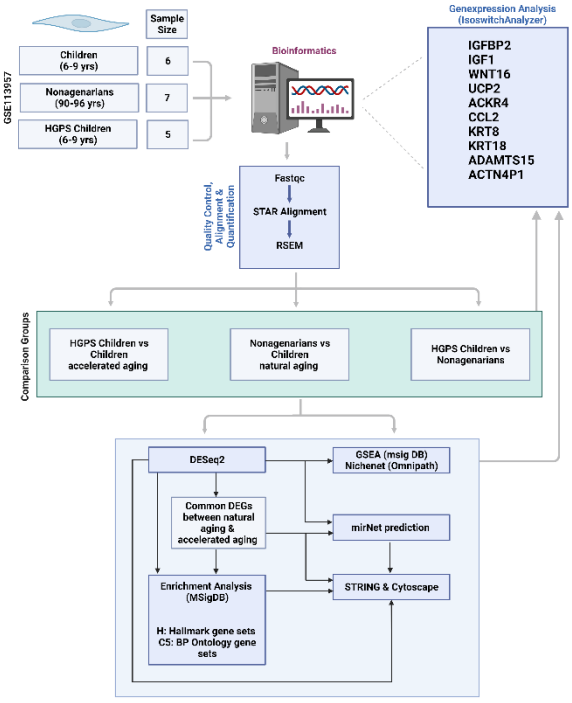

Keywords: progeria; aging; omics; RNA Sequencing; bioinformatics; sun exposure; HGPS; IGFBP2; ACKR4; WNT

1. Introduction

 doi:10.20944/preprints202207.0038.v1

Aging is characterized as a time-dependent functional decline leading to progressive loss of physiological functions and deterioration [1]. It is known as the primary risk factor for several major pathologies, including cardiovascular disorders, diabetes, neurodegenerative diseases, and cancer [1].

López-Otín et al. have defined the hallmarks of aging, aiming for a similar effect on aging research as Hanahan and Weinberg's hallmarks of cancer had on cancer research by contributing to the momentum cancer research has gained in the last decades [1]. The technical progress in research, which becomes obvious by looking at disciplines such as "-omics", also contributes to the growing knowledge and understanding of the processes involved in aging. In general, the ending "-omics" indicates a global or comprehensive assessment of a kind of molecule [2].

Like the first "omics" discipline, genomics, which focuses on entire genomes instead of solely studying single genes [2], all kinds of "-omics" focus on a global or comprehensive assessment of a certain kind of molecule [2]. Transcriptomics, for instance, analyzes RNA levels in a qualitative and quantitative manner [2]. By comparing high-throughput sequencing data of healthy individuals and individuals affected by a disease, it is possible to gain a better understanding of various human pathologies including ageing-related diseases.

An example of the progress in aging research is the rare and fatal premature aging syndrome progeria (Hutchinson-Gilford progeria syndrome, HGPS). The disease was first described in 1886 by Hutchinson [3] and in 1897 by Gilford [4], and was brought to attention as a detailed case study in 1913 [4], emphasizing the need for further knowledge and research [4,5].

Progeria is often diagnosed relatively early in childhood, and as the name suggests, several of the symptoms of progeria also occur with old age, including hair graying or loss, skin thinning, and osteopenia/osteoporosis [6] as well as diminished joint mobility [7]. Besides aging symptoms, progeria patients often suffer from cardiovascular problems [8] as well as stroke [8], which result in premature death and an average life expectancy of about 13 years.

In 2003, 90 years after progeria was ardently brought to attention, a mutation in LMNA was identified as the cause of HGPS by the Progeria Research Foundation's collaborative research team [9]. Due to a dominant 1824C>T mutation, which was found to be the predominant cause of progeria, a cryptic splice donor site gets activated [10,11]. This is causing the formation of a truncated prelamin A, named progerin, which is missing 50 amino acids due to internal deletion and is not processed into normal lamin A [10,11].

Thanks to the efforts of the Progeria Research Foundation (PRF) and the worldwide participation of progeria patients and their families, less than two decades later, two successful clinical trials aiming to treat HGPS and increase the life expectancy of HGPS patients have been performed [12,13] and a third trial is expected to be completed in 2023 (NCT02579044). Additionally, the first medication against progeria has been FDA approved [14] and is in the process of being approved in Europe [15]. Besides searching for a cure, the PRF also supports progeria and aging research by other scientists, for instance, by sharing fibroblasts that were donated by HGPS patients [16,17].

Using human fibroblasts, Fleischer et al. generated a comprehensive set of genome-wide RNA-Seq profiles to develop a computational method to predict the biological age [16,17]. The dataset contains RNA-Seq data of dermal fibroblasts donated by ten progeria patients and 133 "apparently healthy" individuals (aged 1 to 96 years according to their metadata) [16,17]. Their dataset is publicly available on the Gene Expression Omnibus (GEO) database [18] under accession number GSE113957 [16,17] Since its publication in November 2018, the article by Fleischer et al. has been cited 37 times in PubMed (until May 2022), with 13 of the citing papers mentioning the use of the GSE113957 dataset from the Fleischer et al. paper [19-31] (as described in Table 1). According to the publications in PubMed, the dataset alone contributed to 8 studies investigating aging [20,22-28].

 doi:10.20944/preprints202207.0038.v1

The frequent use of the dataset indicates the broad use and the value of the dataset for research, not only in aging research but also in bioinformatics in general. Keeping in mind that there might be further studies either still in preparation or not indexed in PubMed, the possible applications of the dataset are nowhere near exhausted.

Table 1. Publications listed in PubMed that mention the use of the GSE113957 dataset.

Year	Title	Topic/Aim	Ref.
2020	Epigenetic deregulation of lamina-associated domains in Hutchinson-Gilford progeria syndrome	Progeria research epigenetic changes, understanding progeria pathology (Lamina-associated domains (LADs), DNA methylation, chromatin accessibility changes)	[25]
2020	Phosphorylated Lamin A/C in the Nuclear Interior Binds Active Enhancers Associated with Abnormal Transcription in Progeria	Progeria research understanding progeria pathophysiology (pS22-Lamin A/C-binding)	[20]
2020	Prevalent intron retention fine-tunes gene expression and contributes to cellular senescence	Aging research molecular mechanisms involved in aging (senescence, alternative splicing, intron retention)	[24]
2020	Analysis of transcriptional modules during human fibroblast ageing	Aging research genome-wide transcriptional changes upon aging, potential biomarkers (network-based gene screening, Weighted Gene Co-expression Network Analysis, STRING database, validation via RT-qPCR assay)	[22]
2020	Repetitive elements as a transcriptomic marker of aging: Evidence in multiple datasets and models	Aging research Transcriptomic markers of aging (noncoding repetitive element transcripts, transcriptomic markers of age/aging)	[23]
2021	Altered Chromatin States Drive Cryptic Transcription in Aging Mammalian Stem Cells	Aging research molecular mechanisms involved in aging (age-associated cryptic transcription and chromatin signature)	[28]
2021	Extremes of age are associated with differences in the expression of selected pattern recognition receptor genes and ACE2, the receptor for SARS-CoV-2: implications for the epidemiology of COVID-19 disease	Aging research related to another disease Effect of extreme age on the expression of genes known to interact with SARS-CoV-2	[26]

 doi:10.20944/preprints202207.0038.v1

2022	Multi-omic rejuvenation of human cells by maturation phase transient reprogramming	Aging research/rejuvenation/anti-aging "maturation phase transient reprogramming" (MPTR) method, rejuvenates transcriptome and epigenome	[27]
2021	BiT age: A transcriptome-based aging clock near the theoretical limit of accuracy	Computational method/tool for aging research binarized transcriptomic aging (BiT age) clock estimation/prediction of biological age (genes and transcription factors involved in aging)	[29]
2019	Genome-wide quantification of ADAR adenosine-to-inosine RNA editing activity	Computational method/tool Alu editing index (AEI) quantification of ADAR (adenosine deaminase acting on RNA) activity (e.g., Adenosine-to-inosine (A-to-I) RNA editing)	[21]
2020	mitoXplorer, a visual data mining platform to systematically analyze and visualize mitochondrial expression dynamics and mutations	Computational method/tool visual data mining platform mitoXplorer integrates expression and mutation data of mito-genes with a manually curated mitochondrial interactome (mitochondrial expression dynamics and mutations across various datasets from four model species, including human)	[30]
2021	An integrated pipeline for mammalian genetic screening	Computational method/tool sequencing-based target ascertainment and modular perturbation screening (STAMPScreen) method for enabling cellular engineering (computational method to identify candidate genes for a specific phenotypic conversion using RNA seq data, workflow for the study and engineering of cellular phenotypes)	[19]
2022	Landscape of adenosine-to-inosine RNA recoding across human tissues	Computational method/tool RNA editing detection approach, dedicated and optimized for the coding region RNA editing within the coding sequence can result in amino-acid substitution ("recoding") diversifying the proteome (Adenosine-to-inosine (A-to-I) RNA editing)	[31]

 doi:10.20944/preprints202207.0038.v1

Besides the extensive comparison data for creating and testing computational analysis methods, the RNA seq data can be combined with new analysis methods and the growing knowledge regarding pathways and protein interactions. This will enable further insights and lead to new findings regarding fibroblasts, aging, pathways, and potential relationships and interactions.

In the present study, we used the RNA sequencing data to demonstrate the power of bioinformatics to reveal important differences between normal aging, progeria, and young fibroblasts in terms of pathways, proteins, and protein networks. We considered three subgroups of the dataset: healthy children, nonagenarians, and HGPS patients. As HGPS patients suffer from many conditions associated with old age, we were interested in the differences and similarities between HGPS patients and nonagenarians, as well as between healthy children and children suffering from HGPS. Additionally, we compared the RNA seq data of healthy children and nonagenarians to see the differences in gene expression occurring during natural aging.

All tools used for this analysis are freely available R packages or software. To encourage such analyses for other pathophysiological conditions and stimulate transcriptome analysis, we will give some details on the different tools and where to find vignettes and workflows explaining the use of the respective tools (Supplementary Materials, Document S1).

2. Materials and Methods

In this study, already published, publicly available data is analyzed. Thus, ethical approval and patient consent were not necessary.

2.1. Hardware and Software

All analyzes were performed on a PC with AMD Ryzen 9 3900X, 12-Core Processor, 64.0 GB RAM, 64-Bit-Operating System, and an x64-based processor. A virtual Ubuntu environment (Ubuntu 20.04.2 LTS (OS-Type: 64-bit) running on a virtual machine (Virtual Box 6.1.34)) was used for data download, quality control, and alignment. The subsequent data analysis was performed using RStudio (2022.02.0+443 "Prairie Trillium" Release (9f7969398b90468440a501cf065295d9050bb776, 2022-02-16) for Ubuntu) with R version 4.2.0 (2022-04-22) [32]. Cytoscape analyses were performed using Cytoscape for Windows (64-bit, version 3.9.1, on Windows 10).

2.2. RNA Seq Data

The single-end stranded RNA-Seq data of the GEO [33] dataset GSE113957 was downloaded via NCBI's SRA Run Selector and checked for quality using FastQC (version 0.11.9) [34] and MultiQC (version 1.12) [35]. The dataset was generated by Fleischer et al. [16,17] . It contains RNA seq data of human fibroblast cell lines derived from 10 progeria patients (Hutchinson-Gilford progeria syndrome (HGPS)) and 133 fibroblast cell lines derived from "apparently healthy" individuals [16,17]. According to the metadata provided via NCBI's SRA Run Selector, the healthy individuals were aged between 1 to 96.

For this study, only the samples of the progeria patients aged 6 to 8 years (5 samples), the samples of healthy children in the same age group (age 6 to 9, 6 samples), and the samples of the individuals aged 90+ (7 samples) were analyzed.

2.3. Data Preprocessing

The RNA-seq data was aligned to GENCODE v39 [36] using the standard protocols for STAR (version 2.7.10a) [37] and RSEM (version 1.3.1) [38]. After STAR alignment, the transcripts were subsequently quantified with RSEM.

 doi:10.20944/preprints202207.0038.v1

2.4. Identification of DEGs

We performed DESeq2 (version 1.36.0, with apeglm version 1.18.0, using tximport version 1.24.0 for importing the data in R) [39-41] analyses to find differences between the two groups: (1) HGPS patients vs. healthy children and (2) 90-year-olds vs. healthy children. Differentially expressed genes (DEGs) with a p-value < 0.05 were considered significant. The log2 fold change threshold values were set to > 1 for upregulated genes and < -1 for downregulated genes.

2.5. Data Visualization

Principal component analysis (PCA) was performed using the DESeq2 package, and gene expression and DEGs were visualized in the form of volcano plots (EnhancedVolcano, version 1.14.0) [42] and heatmaps (pheatmap version 1.0.12) [43].

Additionally, gene expression was visualized using IsoformSwitchAnalyzeR (version 1.18.0) [44], which supports data from various quantification tools, including RSEM [44]. To calculate gene expression, IsoformSwitchAnalyzeR can take count and abundance values into account and calculates gene expression by adding up the abundance values of all isoforms related to the respective gene [44]. The gene expression function of the IsoformSwitchAnalyzeR package was used for three different comparisons: (1) HGPS patients vs. healthy children, (2) 90-year-olds vs. healthy children, and (3) HGPS patients vs. 90-year-olds.

2.6. Pathway Enrichment Analysis

Databases such as the Molecular Signatures Database [45-48], provide annotated gene sets that can be used for further analyses, including hallmark gene sets and ontology gene sets. The hallmarks gene set can be envisioned as a starting point for further analyses [46]. Biological ontologies, such as the Gene Ontology (GO) [47], provide knowledge about genes and their functions [49,50]. The gene ontology offers information on the sub ontologies that represent protein function: biological process (BP), cellular component (CC), and molecular function (MF) [51].

The enrichment analyses of the hallmark gene set and the GO BPs gene set were calculated using MSigDB (version 7.5.1) [45-48], and visualized as bar plots, CNET plots, and heat plots using clusterProfiler (version 4.4.2) [49,52], enrichplot (version 1.16.1) [53], and ggplot2 (version 3.3.6) [54]. The heat plot function of the enrichplot package [53], which is also embedded in clusterProfiler [49,52], combines the functionalities of a heatmap and a CNET plot by displaying relationships, for instance, the genes involved in a specific pathway, as a heatmap [53].

2.7. Protein-protein Interactions

The Search Tool for Retrieval of Interacting Genes/Proteins (STRING) database [55] and web tool is a meta-resource for analyzing protein-protein interactions [55,56]. It is based on analyzing the 'functional association' of proteins, which is described as a link between two proteins that both contribute to a biological function [55].

The significant DEGs of interest were mapped to STRING using the official gene symbol as input for the web app (https://string-db.org/, version 11.5) with a fullstringnetwork medium confidence of 0.4 and visualized via Cytoscape [57].

The open-source software project Cytoscape was developed as a modeling environment for the integration of molecular network interaction data. Its organizing metaphor is a network graph [57]. The nodes of the graph are molecular species that are connected via intermolecular interactions, which are represented as edges or links between the nodes. It supports various automated network layout algorithms and allows the user to visualize their data in the form of a network [57]. Furthermore, Cytoscape is designed to allow the implementation of additional plug-ins addressing biological problems [57].

 doi:10.20944/preprints202207.0038.v1

We used Cytoscape [57] to further analyze and visualize the STRING database results for our genes of interest. Additionally, using Cytoscape [57], we visualized the log2fold changes of the DEGs that were calculated during DESeq2 analysis [39] (for aging and progeria) and the average log2fold changes of the common DEGs in both conditions (calculated by adding the respective values and subsequently dividing them by 2).

2.8. Venn Diagrams

Venn diagrams were introduced almost 150 years ago as a method of visually representing classes and elements contained in one or several of these classes using intersecting circles [58]. Venn Diagrams can represent results that are rather difficult to explain in words in an intuitively understandable graphic representation. Therefore, they can be used to visualize overlapping genes between several groups. Besides that, Venn diagram tools, like the web app Venny [59] (https://bioinfogp.cnb.csic.es/tools/venny/), also offer to extract lists of every section of the Venn diagram [59].

The different genes of interest for the respective groups were visualized using the online tool Venny (version 2.1.0) [59]. Depending on the comparison, two or three lists of DEGs or pathways were uploaded in Venny, which automatically visualized overlaps and offers the option to save the resulting figure and the elements contained in the overlaps.

2.9. miRNA prediction

For predicting miRNA interactions, we used miRNet (https://www.mirnet.ca/, version 2.0), a web-based platform for miRNA analysis. The input data is integrated with prior knowledge, including miRNA-target interactions, transcription factors, and single nucleotide polymorphisms [60], and the results can be visualized as a network using Cytoscape [57]. This allows for predicting miRNAs that might be regulated by genes of interest. We performed three miRNA predictions, using the DEGs involved in aging, progeria, and the common DEGs of both conditions as the respective input data.

2.10. NicheNet: Finding Ligand-Receptor-Interactions Based on Prior Knowledge

Since the growing knowledge of biological processes such as gene interactions and cellular communication is a cornerstone in data analysis, Türei et al. generated Omnipath, a comprehensive database combining over a hundred different resources covering protein interaction, transcriptional and post-transcriptional regulation, and cellular signaling [61].

NicheNet is a computational method developed for combining the prior knowledge archived in databases such as Omnipath with gene expression data, enabling the user to analyze prioritized ligand-target interactions as well as intracellular signaling [62]. Although NicheNet offers its own database, it can also be combined with other databases as the source of the prior knowledge on which the subsequent NicheNet analysis is based.

In this study, we followed the workflow for combining NicheNet (version 1.1.0) [62] and Omnipath data (via OminpathR, version 3.4.0) [61] previously described by Türei et al. [61]. The workflow allows predicting prioritized interaction partners for DEGs involved in a pathway of interest (via fgsea, version 1.22.0) [63], which can offer further insights in network analysis [61].

2.11. Figures and Additional Packages

While the graphical abstract was created using BioRender (https://biorender.com/), the figures containing analyses results were arranged using R/RStudio. The following helpful R packages were used for figure creation or as additional packages/dependencies of the packages used for analyses and figure creation: cowplot (version 1.1.1) [64], ggplotify (version 0.1.0) [65], magick (version 2.7.3) [66], scatterplot3d (version 0.3.41) [67], scales (version 1.2.0) [68], viridis (version 0.6.2) [69], plotly (version 4.10.0) [70], RColorBrewer (version 1.1.3) [71], ggupset (version 0.3.0) [72], ggnewscale (version 0.4.7) [73], pathview (version 1.36.0) [74], ggridges (version 0.5.3) [75], europepmc (version 0.4.1) [76],

 doi:10.20944/preprints202207.0038.v1

BiocManager (version 1.30.18) [77], org.Hs.eg.db (version 3.15.0) [78], tidyverse (version 1.3.1) [79], dplyr (version 1.0.9) [80].

3. Results

HGPS patients suffer from old age symptoms, therefore, we were interested in the differences and similarities of natural, chronological aging, as seen in individuals of extreme age like nonagenarians, and premature or accelerated aging, as it can be observed in progeria patients. For our study, we compared three subsets of the RNA sequencing data within Fleischer et al.'s publicly available GEO dataset GSE113957 [16,17]: HGPS patients, nonagenarians (90s, aged 90 to 96 according to the metadata submitted with the GEO dataset [17]), and healthy children (Supplementary Materials, Table S1). To find genes related to aging and aging-related pathologies, we performed DESeq2 analyses comparing healthy children with progeria patients and nonagenarians, respectively. The results of both analyses were compared, focusing on DEGs, GO enrichment/pathways, miRNAs, and interaction partners.

Since Gordon et al. reported that death due to complications of HGPS such as cardiac or cerebrovascular disease most often occurs in the age range between six and 20 years [81], we decided to focus on children suffering from HGPS aged six or older (HGPS, ages 6 to 8 years). RNA sequencing data samples of healthy children of the same age group (Healthy Kids, aged 6 to 9) were used as controls.

3.1. Differences and Similarities between Old Age and HGPS

The gene expression of HGPS patients (Figure 1) and nonagenarians (Figure 2) were compared with the gene expression of healthy children using DESeq2 analysis [39].

Principal Component Analysis (PCA, Figure 1A, Figure 2A) indicates differences in gene expression between HGPS patients and healthy children (progeria, premature or accelerated aging) and nonagenarians and healthy children (aging), respectively. DEGs are visualized as volcano plot [42] (Figure 1B, Figure 2B) and as heatmap [43] with hierarchical clustering (Figure 1C, Figure 2C). Upregulation is visualized in red, downregulation in blue. Comparing HGPS patients and healthy children (HGPS vs. healthy children, Figure 1) resulted in 497 DEGs, with 332 genes being upregulated and 165 downregulated in progeria. In natural aging (90s vs. healthy children, Figure 2), 2743 genes are differentially expressed, with 1350 DEGs being upregulated and 1393 being downregulated (Supplementary Materials, Table S2).

Hallmark enrichment analysis and Gene Ontology enrichment analysis for biological processes (BPs) were conducted using clusterProfiler [49,52] and the respective gene sets available via the Molecular Signatures Database (MSigDB) [45-48]. While normal aging (Figure 2D and E, Supplementary Materials Figure S3 and S4) appears to affect the cell cycle G2/M checkpoint (G2M checkpoint), E2F targets, and the mitotic spindle assembly (hallmark MITOTIC_SPINDLE), progeria is only associated with KRAS signaling up, the genes upregulated by KRAS (Kristen rat sarcoma virus) activation (Figure 1D and E, Supplementary Materials Figure S1 and S2).

GO enrichment analysis, which was conducted using clusterProfiler [49,52], for BPs using the respective DEGs indicates which BP pathways might be affected by the differences in gene expression. In accelerated aging, 171 BP pathways were significantly enriched. The top ten enriched pathways of the clusterProfiler analysis are visualized as bar plots in Figure 1E. Here, pathways related to skin and skin development are among the top enriched pathways. Among the 189 significantly enriched BP pathways found in natural aging, several pathways related to the cell cycle were among the top ten enriched pathways (Figure 2E). The top three pathways of both comparisons and their related DEGs are visualized as CNET plots in the Supplementary Materials (progeria in Figure

Preprints (www.preprints.org) | NOT PEER-REVIEWED | Posted: 4 July 2022 doi:10.20944/preprints202207.0038.v1

S2, aging in Figure S4), demonstrating that these processes are also interconnected via the involved DEGs.

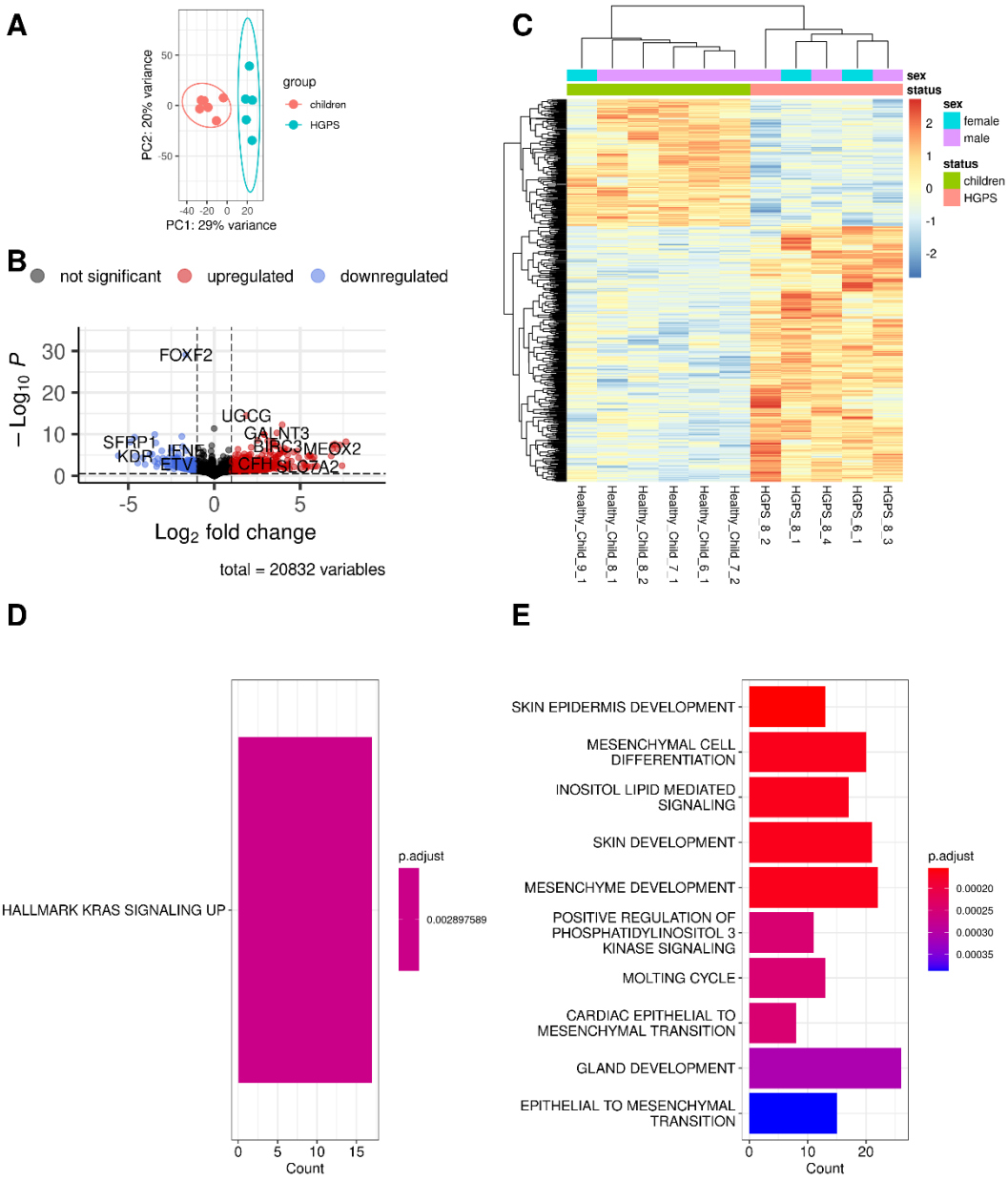

Figure 1. Comparing gene expression in RNA sequencing data of HGPS patients and healthy children (progeria/accelerated aging). **(A)** Principal Component Analysis (PCA): HGPS patients (blue dots) compared to healthy children (controls, red dots) **(B)** Volcano plot visualizing differentially expressed genes (DEGs): significantly upregulated genes are shown as red dots, significantly downregulated genes as blue dots, gray dots symbolize genes without significant changes in gene expression **(C)** Heatmap and hierarchical clustering of the DEGs. **(D)** Bar plot of enriched hallmark pathways. **(E)** Bar plot of GO enriched biological processes.

Preprints (www.preprints.org) | NOT PEER-REVIEWED | Posted: 4 July 2022 doi:10.20944/preprints202207.0038.v1

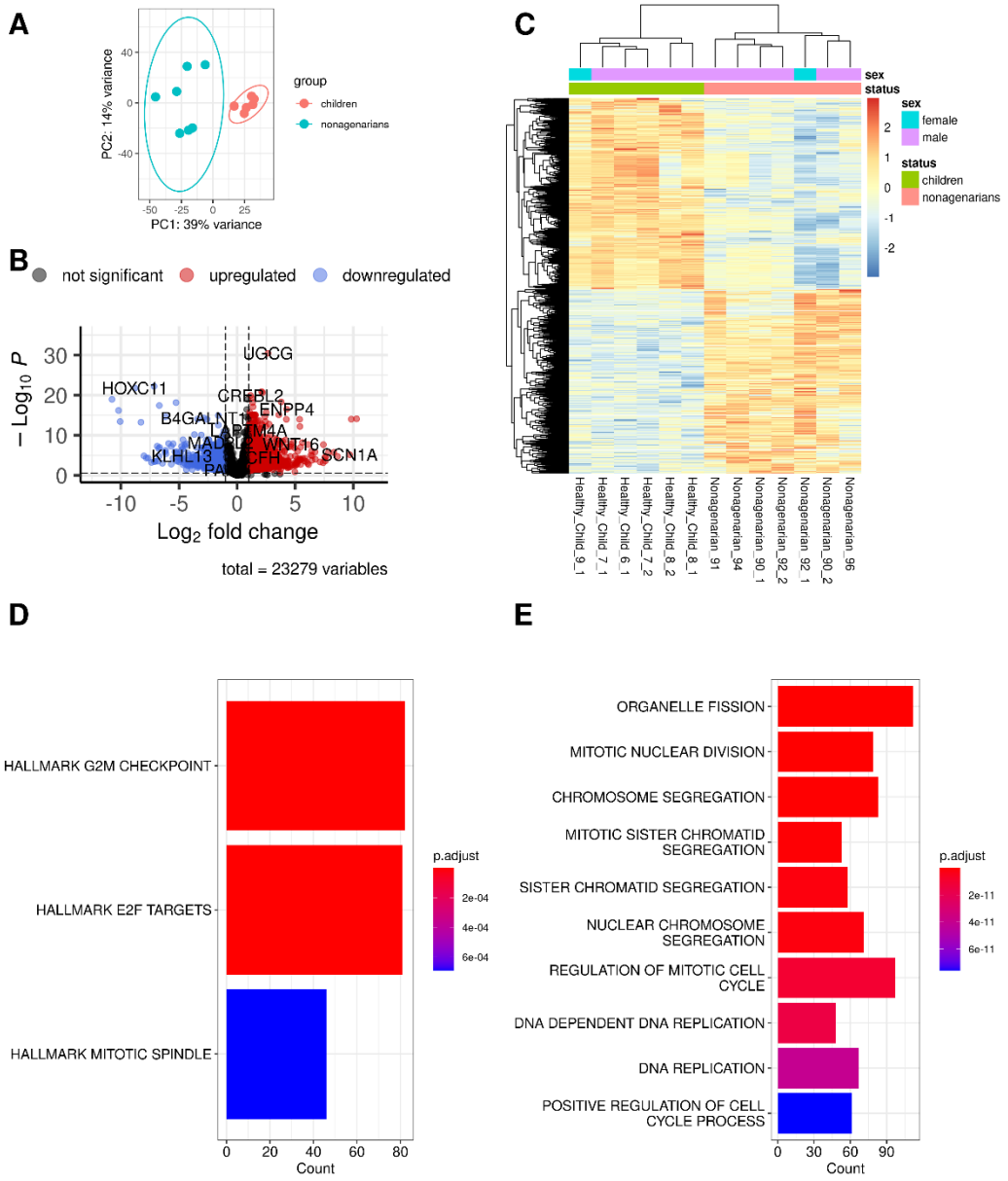

Figure 2. Comparing gene expression in RNA sequencing data of nonagenarians and healthy children (normal/chronological aging). **(A)** Principal Component Analysis (PCA): nonagenarians (blue dots) compared to healthy children (controls, red dots). **(B)** Volcano plot visualizing differentially expressed genes (DEGs): significantly upregulated genes are shown as red dots, significantly downregulated genes as blue dots, gray dots symbolize genes without significant changes in gene expression. **(C)** Heatmap and hierarchical clustering of the DEGs. **(D)** Bar plot of enriched hallmark pathways. **(E)** Bar plot of GO enriched biological processes.

3.2. Changes in Gene Expression in Progeria and Normal Aging

Accelerated and natural aging share changes in gene expression. The Venn diagram in Figure 3A shows that both comparisons have 157 DEGs in common. However, not all of these DEGs are regulated in the same direction in both comparisons. The differences in gene expression of the six differently regulated genes (Figure 3C to E) are visualized using the R-package IsoformSwitchAnalyzeR [44].

Comparing the changes in gene expression (log2foldchanges) of the 157 DEGs revealed that six DEGs (KRT18, KRT8, ACKR4, UCP2, ADAMTS15, and ACTN4P1) were regulated in opposite directions. For instance, while HGPS patients express more KRT18 than healthy children (Figure 3D), the expression of KRT18 appears to be reduced upon

 doi:10.20944/preprints202207.0038.v1

normal aging as nonagenarians express less KRT18 than both healthy children (Figure 3C) and children affected with HGPS (Figure 3E).

Performing GO enrichment with the 157 DEGs that both types of aging have in common results in 27 biological processes. The top ten enriched biological processes of the clusterProfiler analysis using the common DEGs are visualized in Figure 3B. Considering the common DEGs, Epithelial Cell Proliferation (ECP) appears to be the most enriched pathway. Additionally, ECP is also enriched in both comparisons, although it is not among the top ten enriched BPs in accelerated and normal aging.

Comparing the DEGs in HGPS that are involved in ECP with the DEGs in old age and ECP shows that both groups have 15 genes of the ECP pathway in common: WNT16, CCL26, HGF, PTPRN, CCL2, WNT5A, STAT1, IRF6, GDF5, SIX1, KDR, FST, KIT, NKX3-1, and WNT10B (Figure 4A). Analyzing these genes in the STRING database [56] (Figure 4B) shows that almost all of these DEGs are linked with each other.

Further analysis in Cytoscape [57] by combining the STRING results and the changes in gene expression that were evaluated. Cytoscape allows visualizing the ECP-related DEGs. Figure 4C visualizes the ECP-related DEGs both conditions have in common with ECP (octagons) and the ECP-related DEGs specific for comparing HGPS patients and healthy children (rectangles). The log2foldchanges derived from the DESeq2 analysis are indicated by color, with blue symbolizing downregulation and red upregulation. The same analysis was performed comparing the ECP-related common DEGs of both conditions and the DEGs that are related to ECP but only differentially expressed between nonagenarians and healthy children (Supplementary Materials, Figure S5).

Preprints (www.preprints.org) | NOT PEER-REVIEWED | Posted: 4 July 2022 doi:10.20944/preprints202207.0038.v1

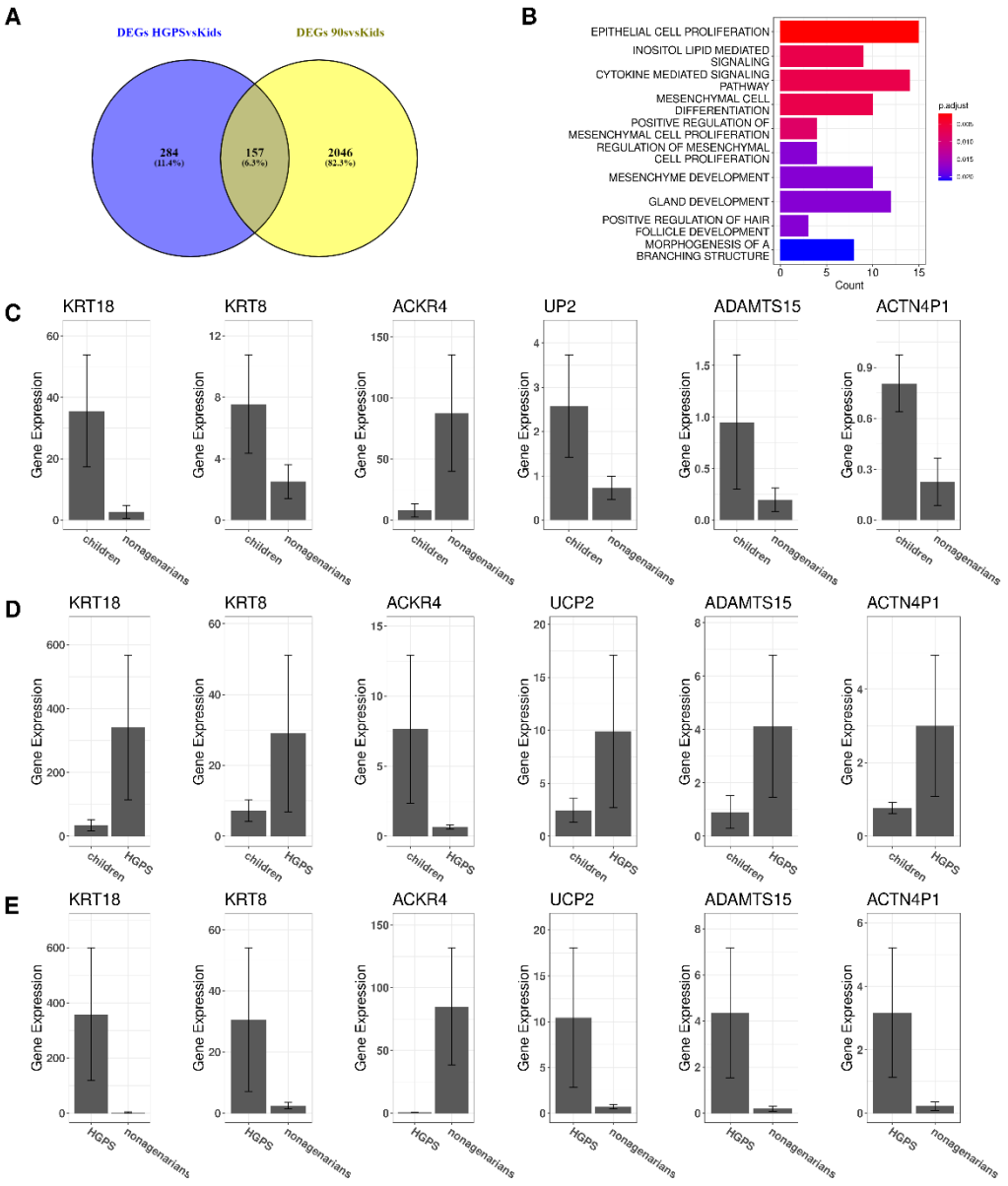

Figure 3. Comparison of accelerated and natural aging. **(A)** Common DEGs in accelerated aging (DEGs between HGPS patients and healthy children, blue) and normal aging (DEGs between nonagenarians and healthy children, yellow) are visualized as Venn diagram. **(B)** The ten most enriched biological processes with GO enrichment using the common DEGs of aging and HGPS (overlap in A). **(C)** Gene expression of the six genes regulated in opposite directions, differences in gene expression between children and nonagenarians. **(D)** Gene expression of the six genes regulated in opposite directions, differences in gene expression between children and progeria patients. **(E)** Gene expression of the six genes regulated in opposite directions, differences in gene expression between progeria patients and nonagenarians.

Preprints (www.preprints.org) | NOT PEER-REVIEWED | Posted: 4 July 2022 doi:10.20944/preprints202207.0038.v1

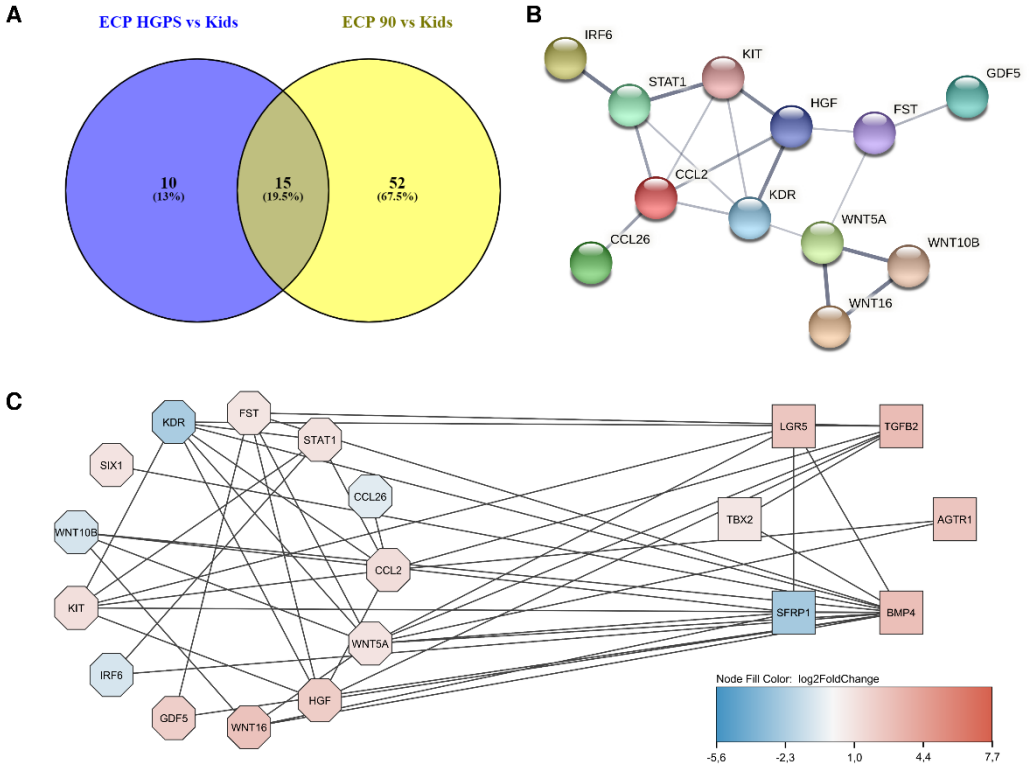

Figure 4. Comparison of accelerated and natural aging. **(A)** The visualization of the DEGs involved in Epithelial Cell Proliferation (ECP) differentially expressed in HGPS (blue) and old age (yellow) shows that both have 15 DEGs in common. **(B)** The common DEGs of old age and HGPS involved in ECP are visualized as STRING network (applying fullstringnetwork medium confidence of 0.4). **(C)** Visualization of the DEGs involved in ECP (by using STRING database and Cytoscape): common DEGs (octagons) and DEGs specific for HGPS (rectangles) and the respective log2foldchanges (blue downregulated, red upregulated).

3.3. The Different Pathways Involved in Progeria, Aging, and Both Conditions

The Venn diagram in Figure 5A visualizes the BPs which were calculated for progeria (Figure 5A, blue circle), aging (Figure 5A, yellow circle), and the DEGs both conditions have in common (Figure 5A, green circle). The complete list of the respective BPs is available in the Supplementary Materials (Table S3).

To compare the changes in gene expression between progeria and aging, we analyzed the 15 common pathways as heat plots (Figure 5B and Figure 5C). The y-axes show the 15 common pathways, while the genes involved in the respective pathways are indicated on the x-axes. The changes in gene expression were derived from the log2fold changes in gene expression in aging (Figure 5B) and progeria (Figure 5C), respectively.

Many genes show similar gene expression patterns and only differ in the log2fold-changes in gene expression. However, some genes are upregulated in one of the comparisons and downregulated in the other (see Figure 3C to E). One of these genes, UCP2, is also involved in gland development. While UCP2 is upregulated in progeria, it is downregulated in nonagenarians. ACKR4, which is also regulated in different directions, is involved in the cytokine-mediated signaling pathway.

Preprints (www.preprints.org) | NOT PEER-REVIEWED | Posted: 4 July 2022 doi:10.20944/preprints202207.0038.v1

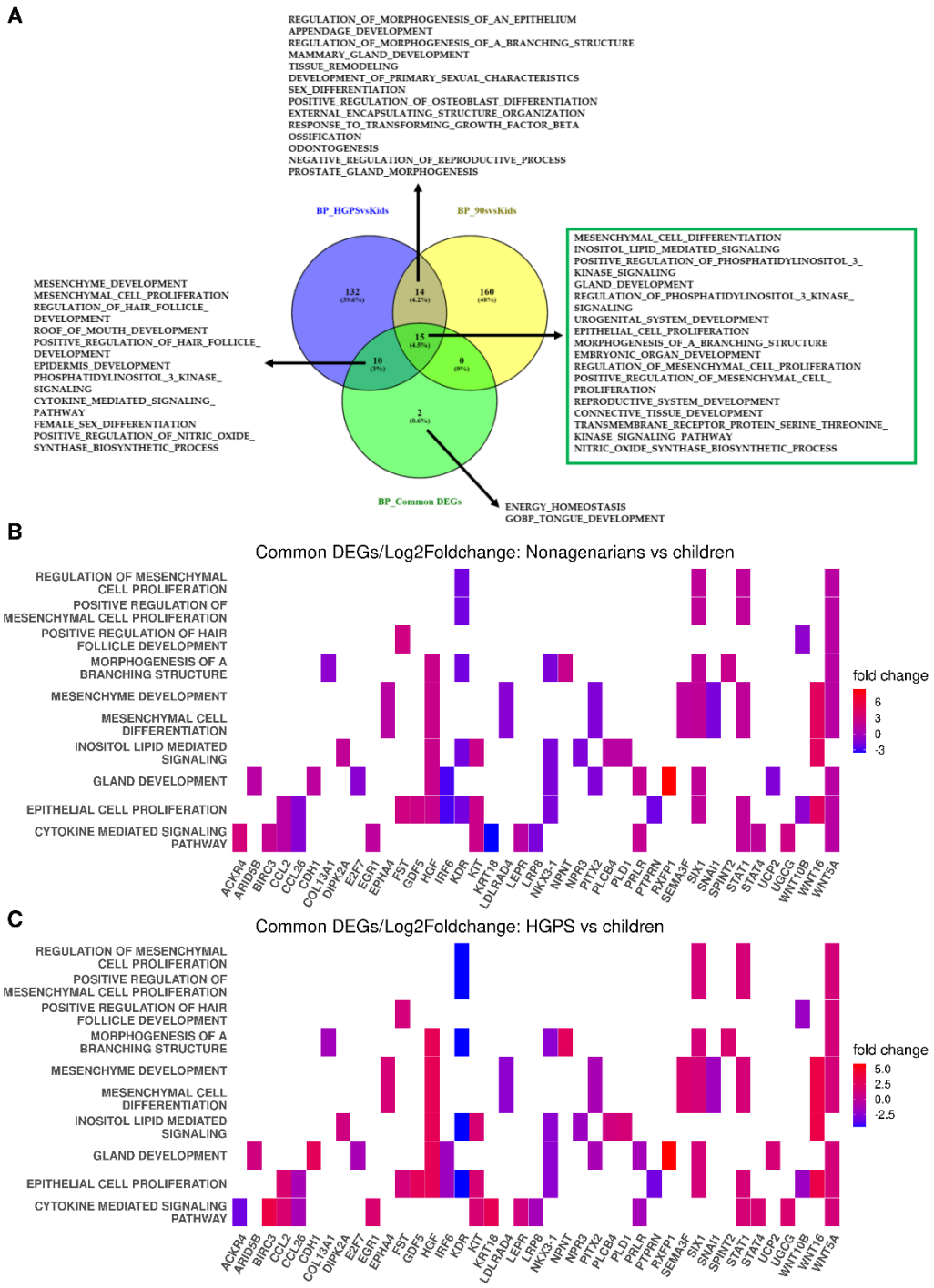

Figure 5. Differences in gene expression between HGPS and aging. **(A)** Venn diagram visualizing the GO BPs enriched in HGPS (blue), aging (yellow), and in the 157 common DEGs of progeria and aging. 15 BPs are enriched in all three analyses. **(B)** Heat plot visualizing the changes in gene expression in the DEGs involved in the 15 BPs using the changes in gene expression observed while comparing nonagenarians and healthy children (log2foldchanges of DESeq2 analysis). **(C)** Heat plot visualizing the changes in gene expression in the DEGs involved in the 15 BPs using the changes in gene expression observed while comparing progeria patients and healthy children (log2foldchanges of DESeq2 analysis). The differences in gene expression are indicated by color (red for upregulated, blue for downregulated). Notably, UCP2, which is involved in gland development, is upregulated in progeria but downregulated in aging. ACKR4, which is involved in the cytokine-mediated signaling pathway, is upregulated in aging (comparison of healthy children and nonagenarians) but downregulated in progeria (comparison of healthy children and progeria patients).

 doi:10.20944/preprints202207.0038.v1

The aging pathway was among the enriched pathways in aging but not in progeria. As we were especially interested in aging, we compared the DEGs of HGPS and aging with the genes known to be involved in the biological process "GOBP_AGING" (Figure 6A), which can be found in the Molecular Signatures Database (MSigDB) [82]. The DEGs between healthy children and nonagenarians also related to the aging pathway are shown in Figure 6B. The three DEGs that appear to be associated with the aging pathway, progeria and normal aging are highlighted in purple.

Besides UCP2, only WNT16 and IGFBP2 are DEGs in both conditions and are known to be involved in the aging pathway. Figure 6C, D, and E visualize the gene expression of the respective genes. Expression of WNT16 is higher in nonagenarians (Figure 6C) and progeria patients (Figure 6D) compared to healthy children. Comparing nonagenarians to progeria patients shows that nonagenarians have a slightly higher expression of WNT16 than HGPS patients (Figure 6E).

Nonagenarians express higher levels of IGFBP2 than healthy children (Figure 6C). Progeria patients present a higher IGFBP2 expression than healthy children (Figure 6D) and even higher IGFBP2 levels than nonagenarians (Figure 6E). Healthy children (Figure 6C) and progeria patients (Figure 6E) express more UCP2 than nonagenarians. At the same time, progeria patients have higher UCP2 levels than healthy children (Figure 6D).

Preprints (www.preprints.org) | NOT PEER-REVIEWED | Posted: 4 July 2022 doi:10.20944/preprints202207.0038.v1

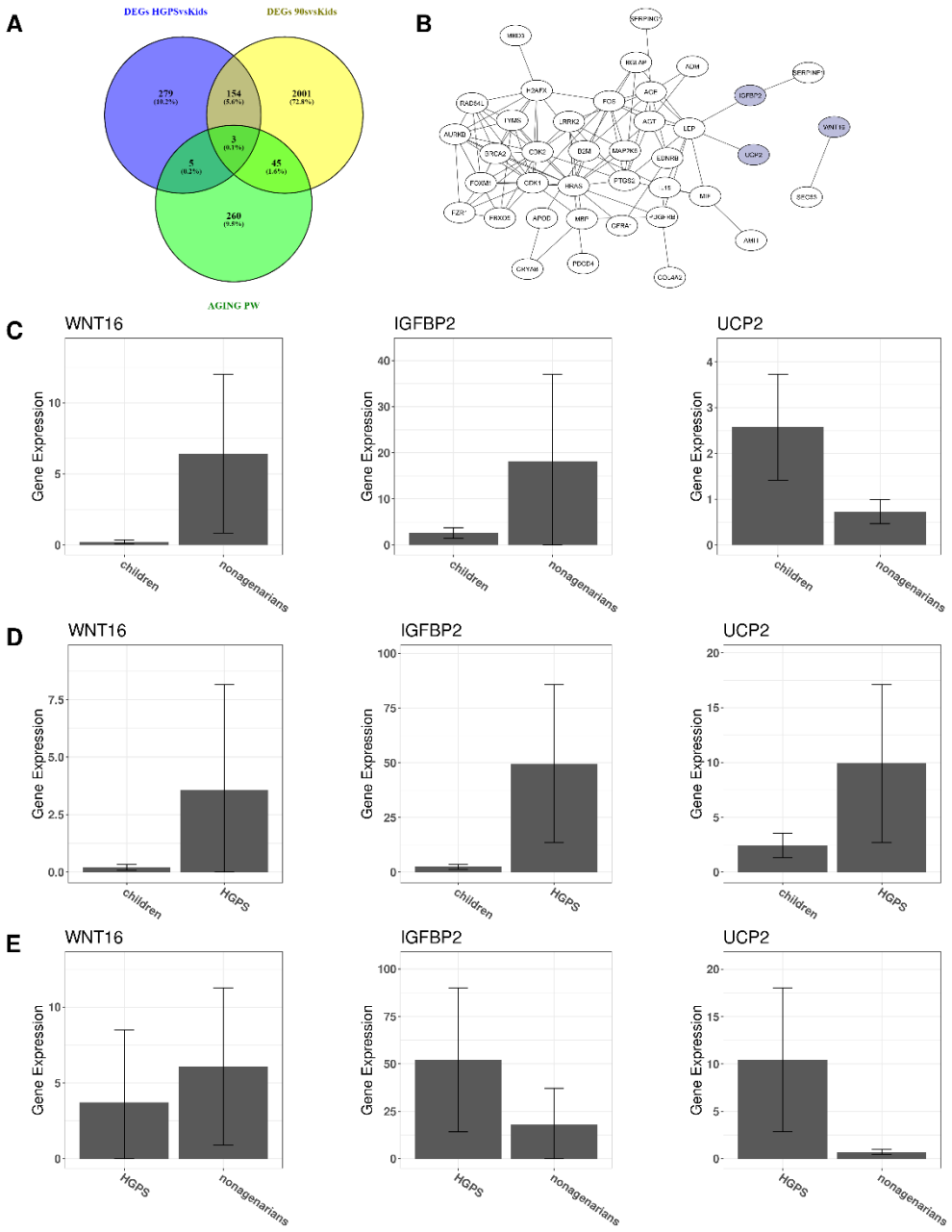

Figure 6. Network visualization of miRNAs related to WNT16, IGFBP2, and UCP2. **(A)** Comparing the genes involved in the Aging Pathway (green) with the DEGs in progeria comparison (blue) and the aging comparison (yellow) results in three common DEGs WNT16, IGFBP2, and UCP2. **(B)** Network visualization of the DEGs involved in the aging pathway and differentially expressed between healthy children and nonagenarians. The three DEGs that are also differentially expressed when comparing progeria patients and nonagenarians are highlighted in purple. **(C)** Gene expression of the three DEGs WNT16, IGFBP2, and UCP2, when comparing children and nonagenarians. **(D)** Gene expression of the three DEGs WNT16, IGFBP2, and UCP2, when comparing children and HGPS patients. **(E)** Gene expression of the three DEGs WNT16, IGFBP2, and UCP2, when comparing progeria patients and nonagenarians.

3.4. Prediction of microRNAs and Visual Exploration of Interaction Partners of WNT16, IGFBP2, and UCP2

MicroRNAs (miRNAs, miRs) are small non-coding RNAs that are photogenically conserved and act as master regulators of gene expression [83]. miRNAs were predicted using the web platform miRNet 2.0 [60]. For our analysis, we used the genes that were differentially expressed in the respective analyses. The predicted miRNAs for all three

 doi:10.20944/preprints202207.0038.v1

analyses (progeria DEGs, aging DEGs, and the 157 common DEGs) and the subsequent analyses are available in the Supplementary Materials (Table S4). Here, we focus on the miRNA prediction using the 157 common DEGs, resulting in 37 predicted miRNAs.

The calculated network of these miRNAs and their interaction partners were imported to Cytoscape for further analysis and filtered for DEGs. The three common aging-related DEGs (WNT16, IGFBP2, and UCP2) revealed five predicted miRNAs: WNT16 is associated with one miRNA (hsa-mir-181a-5p), UCP2 is associated with two miRNAs (hsa-mir-26a-5p and hsa-mir-124-3p), and IGFBP2 is associated with three miRNAs (hsa-mir-124-3p, hsa-mir-126-3p, and hsa-mir-27b-3p). The same five miRNAs were predicted for aging and progeria (Supplementary Materials, Table S4 and Figures S6 to S8).

The miRNAs and their interaction partners of the 157 common DEGs are visualized in Figures 7A to C. Figure 7A shows hsa-mir-181a-5p and its interaction partners, with WNT16 being highlighted. The interaction partners of the three miRNAs associated with IGFBP2 (highlighted) are visualized in Figure 7B, and Figure 7C shows hsa-mir-26a-5p and hsa-mir-124-3p, which are both predicted to interact with UCP2 (highlighted), and their interaction partners. In the Supplementary Materials (Figures S6 to S8), we also visualize the interaction partners of these five miRNAs, including the changes in gene expression using the log2foldchanges obtained when comparing HGPS and healthy children and the interaction partners of the miRNAs and the changes in gene expression (log2foldchanges) obtained by comparing nonagenarians and healthy children.

Preprints (www.preprints.org) | NOT PEER-REVIEWED | Posted: 4 July 2022 doi:10.20944/preprints202207.0038.v1

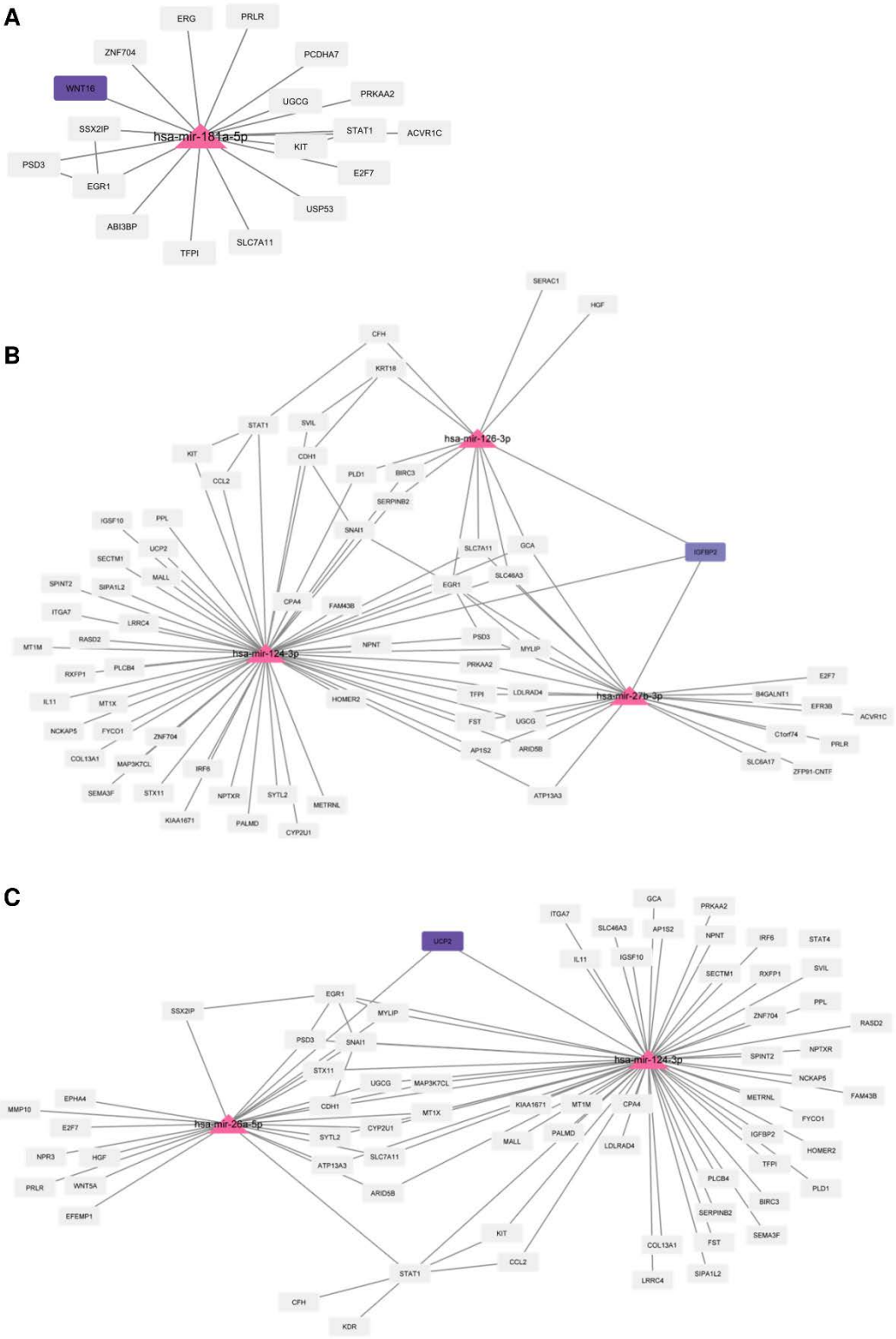

Figure 7. miRNA prediction and network visualization of miRNAs related to WNT16, IGFBP2, and UCP2. **(A)** Predicted interaction partners of hsa-mir-181a-5p, WNT16 is highlighted. **(B)** Predicted interaction partners of hsa-mir-124-3p, hsa-mir-126-3p, and hsa-mir-27b-3p, IGFBP2 is highlighted. **(C)** Predicted interaction partners of hsa-mir-26a-5p and hsa-mir-124-3p, UCP2 is highlighted.

 doi:10.20944/preprints202207.0038.v1

3.5. Predicting Interactions Using NicheNet and Omnipath

Using NicheNet [62] and the Omnipath database [61,84], we combined the experimental results regarding RNA expression obtained from the dataset by Fleischer et al. [16,17] with prior knowledge regarding potential interaction partners from the Omnipath database.

Gene Set Enrichment Analysis (GSEA) [45] is integrated into the NicheNet workflow. Figures 8A and 8E visualize the pathways in aging and HGPS, respectively. The pathway UV response has the highest positive normalized enrichment score (NES) in aging and is also among the top five positive enriched pathways in progeria. Here, we focus on UV response, as it has been shown that sun exposure induces the expression of progerin in human skin [85]. Additionally, accumulation of progerin has been associated with vascular disease in progeria [86], but, over time, it also accumulates in non-HGPS individuals [87]. It might thus contribute to vascular aging and vascular disease [87].

Therefore, the subsequent NicheNet analyses to predict the potential ligand-receptor pairs were performed with UV response as the pathway of interest (Figures 8C, 8D, 8G, and 8H). The Pearson correlation of the predicted ligands involved in UV response is shown in Figures 8B and 8F. Darker color indicates a higher prediction ability. The target genes for these ligands regulating genes related to UV response are visualized as heatmaps for both groups in Figure 8C (comparison nonagenarians and healthy children) and Figure 8G (comparison progeria patients and healthy children). The color intensity indicates the regulatory potential for the top-ranked targets (the 0.1 quantiles) with targets according to the prior model, which was derived from prior knowledge archived in the Omnipath database.

Figures 8C and 8G show the predicted ligand-target interactions. Both analyses have IGF1 and CCL2 as common ligands for the predicted target genes. IGF1 expression is higher in children both compared to nonagenarians (Figure 8I) and progeria patients (Figure 8J). When comparing IGF1 expression in nonagenarians and progeria patients, the expression levels show little difference (Figure 8K).

Predicting the ligand-receptor interactions shows which of the receptors that are expressed in the respective genes might interact with the prioritized ligands. Figure 8D shows the comparison of nonagenarians and healthy children focusing on UV response, Figure 8H shows the comparison of progeria patients and healthy children focusing on UV response.

The only ligand that both analyses have in common is CCL2. CCL2 is an upregulated DEG when comparing nonagenarians and healthy children (Figure 8I). It is upregulated even more when comparing progeria patients and healthy children (Figure 8J). When comparing CCL2 expression in progeria patients and nonagenarians, CCL2 is more expressed in progeria (Figure 8K).

ACKR4 is the only potential CCL2 receptor that is also a DEG in aging and progeria.

To find possible interaction partners of CCL2 that are differentially expressed in both analyses, we uploaded the set of HGPS DEGs obtained by comparing progeria patients and healthy children in STRING. The results of the STRING analysis, the interactions found between the DEGs, were subsequently analyzed in Cytoscape by selecting CCL2 and its neighbors, resulting in a list of DEGs (CCL2-HGPSvsKids, blue circle in Figure 9A). The same steps were repeated using the aging DEGs obtained by comparing nonagenarians with healthy children (CCL2-90svsKids, yellow circle in Figure 9A). The overlapping 16 DEGs of both groups (STAT4, ACKR4, CCL26, CCL2, CFH, HGF, LEPR, SNAI1, CDH1, MSR1, KDR, EGR1, MMP10, KIT, IL11, and STAT1) were visualized in STRING (Figure 9B).

Preprints (www.preprints.org) | NOT PEER-REVIEWED | Posted: 4 July 2022 doi:10.20944/preprints202207.0038.v1

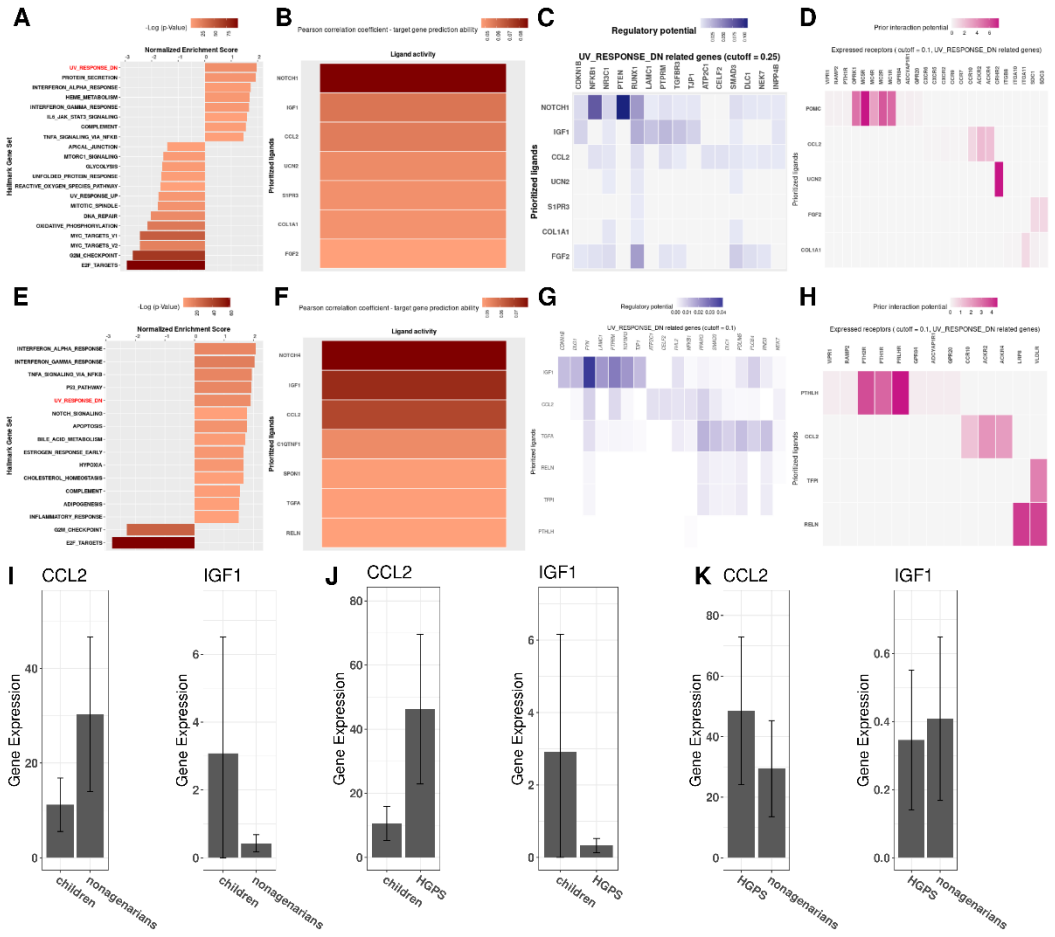

Figure 8. NicheNet analyses of progeria and aging. **(A)** GSEA pathways when comparing nonagenarians and healthy children. **(B)** Pearson correlation of the predicted ligands in the aging comparison. **(C)** Heatmap of predicted ligand-target interactions in the aging comparison. **(D)** Heatmap of the predicted ligand-receptor interactions in the aging comparison and their respective receptors. **(E)** GSEA pathways when comparing HGPS patients and healthy children. **(F)** Pearson correlation of the predicted ligands in the progeria comparison. **(G)** Heatmap of predicted ligand-target interactions in the progeria comparison. **(H)** Heatmap of the predicted ligand-receptor interactions in the progeria comparison. **(I)** Expression of CCL2 and IGF1 in children and nonagenarians. **(J)** Expression of CCL2 and IGF1 in children and progeria patients. **(K)** Expression of CCL2 and IGF1 in progeria patients and nonagenarians.

Preprints (www.preprints.org) | NOT PEER-REVIEWED | Posted: 4 July 2022 doi:10.20944/preprints202207.0038.v1

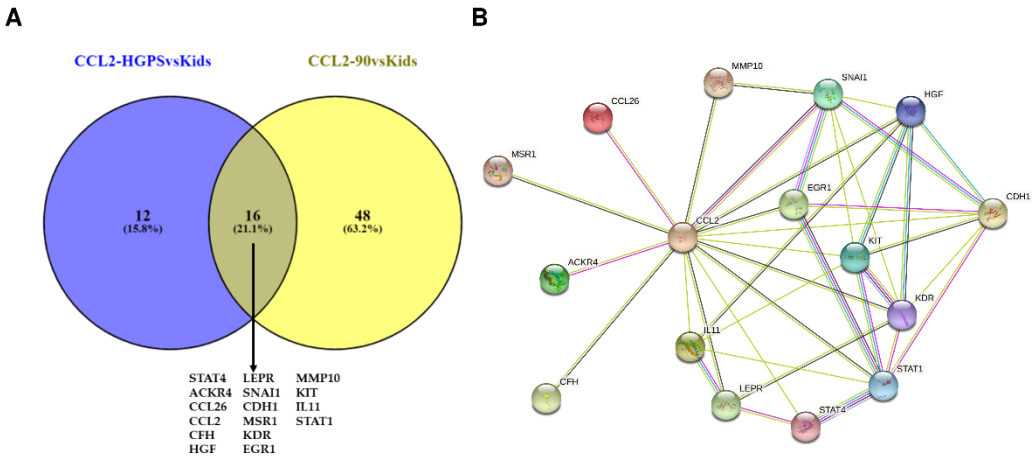

Figure 9. NicheNet and STRING analysis of progeria and aging. **(A)** The 16 common CCL2 interaction partners are the overlapping neighbors of CCL2 in the DEGs of the progeria comparison (blue) and the DEGs of the aging comparison (yellow), respectively. **(B)** STRING network of CCL2 and the 16 CCL2 interaction partners that are differentially expressed in both comparisons.

The STRING analysis shows that all of the DEGs that are part of both analyses have already been associated with CCL2. Several of these DEGs have at least been co-mentioned in PubMed abstracts: Four (KIT, CDH1, STAT4, and IL11) have been co-mentioned in PubMed abstracts, four (MSR1, LEPR2, EGR1, and STAT1) have been co-mentioned and have putative homologs that are co-expressed in other organisms, four (HGF, CFH, MMP10, and KDR) have been co-mentioned and are co-expressed in humans, and one (SNAI1) has been co-mentioned, is co-expressed in humans, and has been associated with CCL2 in experimental/biochemical data. CCL2 and both CCL26 and ACKR4 have been co-mentioned and have experimental/biochemical data suggesting a possible functional link.

Out of the three likely interaction partners of CCL2 (CCR10, ACKR2, and ACKR4) that were predicted using NicheNet and focusing on UV response, only ACKR4 is differentially expressed in both analyses. As ACKR4 was regulated in different directions in progeria and aging (downregulated in HGPS, upregulated in aging, Figure 3C to 3E), ACKR4 might play an important role in both processes and might be involved in the severity of the symptoms or the differences between accelerated and normal aging.

4. Discussion

In 1987, Rowe and Kahn proposed the concept of “successful aging”, pointing out that many of the changes regarded as “normal” during aging are preventable [88]. They also reported that some of these changes could be reversed [88] interpreting “aging as a disease”, a notion that has already been proposed in ancient times [89] and has recently garnered attention [89,90]. Regardless of whether aging should be seen as a disease or not, extending not only the lifespan but also the health span [1,89,90] and possibly even rejuvenation [27] are of great interest. In this study, we analyzed a publicly available RNA Seq dataset using bioinformatic tools.

Although the name “progeria” is derived from Greek for “prematurely old” [4], there are differences in differential gene expression between HGPS and “normal” aging. Gene expression in both groups, the HGPS patients and the nonagenarians, differs from gene expression in the control group of healthy children. However, there are distinct differences between the analysis results for progeria and aging. While both conditions have 157 DEGs in common, there are also DEGs specific to the respective conditions. This results in different biological processes being affected by the changes in gene expression, evident in enrichment analyses.

 doi:10.20944/preprints202207.0038.v1

The differences might be due to differences between progeria patients and nonagenarians. While progeria patients are children suffering from a rare and fatal disease resulting in premature aging [91], the nonagenarians might be examples of "successful aging" [88].

Additionally, enrichment analyses might reveal relevant information for understanding and treating the conditions.

For instance, the only hallmark gene set that is enriched when comparing progeria patients and healthy children is KRAS signaling up. KRAS is known as the most frequently mutated RAS isoform [92]. Due to the oncogenic nature of mutations in the RAS genes, RAS inhibitors such as farnesyltransferase inhibitors (FTIs) have been researched as potential anticancer drugs [92,93], although FTIs did not advance into clinical use due to their lack of efficacy in cancer therapy in clinical trial [93,94]. The similarity in the post-translational processing of RAS and progerin led to the repurposing of FTIs as potential treatments for HGPS [94]. One of these drugs, lonafarnib (zokinvy), was successfully tested as progeria treatment in the first clinical trial for treating progeria [12] and has since been FDA approved [14], becoming the first FDA approved drug for progeria treatment [94].

Since Fleischer et al. obtained the dermal fibroblasts from "apparently healthy individuals" via the Coriell Institute cell repository [16], there is no further information on the donors available. The number of samples (5-7/group) is sufficient for RNA Seq data analysis using DESeq2 [39,95,96]. However, a bigger sample size and detailed medical history of the fibroblast donors could have contributed to further insights.

Here, we focused on the 157 common DEGs in progeria vs aging speculating they should be involved in or at least related to the aging process and might be the key to understanding aging and the processes involved. Surprisingly, six of these DEGs are regulated in different directions in progeria and aging, respectively. Five of the DEGs (KRT8, KRT18, ADAMTS15, ACTN4P1, and UCP2) are upregulated in HGPS patients compared to healthy children and nonagenarians but downregulated when comparing nonagenarians and healthy children.

The sixth DEG, ACKR4, is downregulated in children suffering from progeria compared to healthy children and nonagenarians. Nonagenarians have higher ACKR4 levels than healthy children. The opposite regulation of these genes might lead to a better understanding of the differences between progeria and aging. Furthermore, the regulation of the DEGs could indicate accelerated aging or normal aging.

KRT8 and KRT18 have been linked to modulating cellular stress response and cell resistance to apoptosis [97]. KRT18 has been suggested as a possible biomarker for frailty and aging [98], due to KRT18 and cKRT18 being biomarkers for diseases with apoptotic and mitochondrial defects, which are among the hallmarks of aging, and its association with senescence and anti-mitochondrial auto-antibody formation [98].

The nonagenarians, on the other hand, appeared to have rather low KRT18 expression, although KRT18 levels would be expected to rise with increasing age [98]. If KRT18 expression in fibroblasts is similar to other tissues, this finding might indicate that the nonagenarian fibroblast donors were of extremely good health or that progeria severely affects the skin, which corresponds to skin problems being among the typical progeria symptoms [7,8]. Therefore, examining KRT18 and its interaction partners in HGPS and different age groups might lead to further insights regarding aging and "successful aging".

ADAM metallopeptidase with thrombospondin type 1 motif 15 (ADAMTS15) is upregulated in HGPS but appears to be downregulated upon aging (both compared to healthy children). ADAMTS15, along with ADAMTS1, 4, 5, 9, and 20, is involved in several processes, including palate formation, skin pigmentation, myogenesis, and cardiac development [99], all of which appear to be affected by progeria. In addition, ADAMTS15 is involved in the turnover of cartilage and/or bone during joint inflammation [100] and

 doi:10.20944/preprints202207.0038.v1

the inverse correlation of ADAMTS15 and CITED2 expression links it to the Wnt pathways associated with bone formation and inflammatory arthritis [100].

Thus, ADAMTS15 might be interesting research targets in progeria and aging-related research, especially as WNT16 is among the only three DEGs that progeria, aging, and the aging pathway have in common.

The role of actinin alpha 4 pseudogene 1 (ACTN4P1) is not yet known. Pseudogenes have long been regarded as "void of function" [101] or "junk DNA" [102,103]. However, research has shown that they can affect coding genes and are transcribed into RNA [102,103] and are involved in regulatory functions [103].

Progeria patients had higher ACTN4P1 expression than healthy children in our study and even higher ACTN4P1 expression compared to nonagenarians. To our knowledge, this is the first publication mentioning ACTN4P1, which warrants further investigation of which processes and interaction partners are affected by ACTN4P1 and whether the pseudogene is involved in aging-related processes.

WNT16 is among the DEGs with rather drastic changes in gene expression, indicating that WNT16 might be of special importance in both progeria and aging. This is coherent with literature as Marthandan and colleagues assessed the five most commonly used human fibroblast strains for laboratory use by deep RNA sequencing and real-time PCR and demonstrated that WNT16 and IGFBP2 are among the most differentially expressed genes upon aging [104]. In aging research, WNT16 has already garnered interest due to its association with bone mineral density, bone strength, and fracture risk [105]. WNT16B has been associated with regulating the onset of replicative senescence and belongs to the WNT family, a family of secreted proteins involved in development, aging, senescence, and tumorigenesis [106]. Additionally, it has been proposed that progerin directly affects the transmission of Wnt signaling pathway, which is known to be impaired in HGPS [107]. Our study further confirms a possible connection between Wnt signaling, progeria, and aging.

Another aging related gene, UCP2, is shown as upregulated in progeria compared to healthy children and nonagenarians. Upregulation of UCP2 was observed in aged rats [108] and a mouse model of premature aging [109,110], where UCP2 expression appeared to have metabolic effects [110]. Its upregulation in spontaneously obese mice suggested UCP2 mediated metabolic adaption to the increase of fatty acid biosynthesis and elevated lipid levels [108]. Increased UCP2 expression has been correlated with increased levels of free fatty acids, which is proposed to be involved in downregulating IGF1 levels via a negative feedback loop [108]. Therefore, UCP2 has been associated with counterregulatory effects on aging and age-related pathologies in mice, possibly via modulating the insulin/IGF1 signaling pathway, which indicates that targeted increase of UCP2 levels might prolong the lifespan of mammals [108].

However, in progeria, the high UCP2 levels do not correlate with patients' body weight, as low body weight is one of the characteristics of progeria [8]. In addition, there appear to be parallels between UCP2 and the different LMNA isoforms. A study comparing the effects of lamin A, lamin C, and progerin, the truncated form of lamin A, in mice revealed that progerin and lamin C regulate mitochondrial biogenesis and energy expenditure via triggering antagonistic signals in adipose tissue [111]. While mice only expressing lamin C were obese and had an increased lifespan, the role of progerin in adipose tissue homeostasis might have an opposing effect on lifespan [111]. Additionally, the rather skinny progerin expressing mice were more sensitive to insulin and appeared to have a higher metabolic rate and use more carbohydrates [111]. In contrast, the lamin C expressing mice were moderately insulin-resistant, showed reduced overall energy consumption, and appeared to prefer fatty acids [111]. Involvement of UCP2 in aging and insulin signaling is similar to progerin and of great interest to research further.

Insulin-like growth factor-binding protein 2 (IGFBP2) levels positively correlate with age, insulin sensitivity and inversely correlate with the body mass index (BMI) [112]. Van den Beld et al. conducted a 20-year longitudinal study, repeatedly measuring BMI, IGF1,

 doi:10.20944/preprints202207.0038.v1

IGFBP2, insulin sensitivity, and mortality around the ages of 55, 65, and 75 in 539 participants [112]. They reported, when adjusted for BMI, IGFBP2 levels and insulin sensitivity show a positive correlation [112]. Therefore the authors suggest IGFBP2 as a possible marker for insulin sensitivity [112].

We are, to our knowledge, the first to report and stress these elevated IGFBP2 levels in progeria patients. In our comparative analysis, IGFBP2 levels in healthy children and nonagenarians shows its upregulation with age. However, in progeria, IGFBP2 expression is considerably more elevated than in nonagenarians suggesting its role in both aging and progeria. Such upregulation in progeria could be related to their weight, as children suffering from progeria typically have rather low BMIs [8]. The age-related increase of IGFBP2 levels, especially after 50 [112], could also be connected with the high IGFBP2 expression in accelerated aging and in serum, it appears to be a mortality marker that positively correlated with insulin sensitivity [112].

While pseudogenes such as ACTN4P1 are still garnering research interest [101,102,113,114], microRNAs (miRNAs/miRs), which have been equally disregarded for a long time [115], are increasingly recognized as therapeutic targets [115] and show promising therapeutic results [116]. Hence, we included miRNA prediction, which is a promising research field on its own, in our analyses.

Three of the 37 miRNAs that were predicted using the common DEGs as input might be associated with IGFBP2: hsa-mir-27b-3p, hsa-mir-126-3p, and hsa-mir-124-3p.

In the plasma, hsa-mir-126-3p appears to be upregulated with age [117], while the miRNA was found to be downregulated in blood samples of centenarians and has therefore been proposed as a potential longevity biomarker [117,118]. Olivieri et al. reported that the increase of hsa-mir-126-3p blood level was accompanied by an increase of hsa-mir-126-3p in human endothelial cells during senescence [119]. They also observed lower hsa-mir-126-3p levels in type 2 diabetes mellitus patients and proposed a possible interrelationship between mir-126-3p downregulation and age-related conditions with a pro-inflammatory background, while an increase of mir-126-3p might act as a positive compensatory mechanism [119]. miR-27b expression appears to affect wound healing in skin, as a study by Bi et al. indicates [120]. They reported increased fibroblast proliferation and thus accelerated healing of scald wounds in rats upon miR-27b inhibition [120].

Both IGFBP2 and UCP2 are associated with miR-124, which has been shown to increase in senescent skin and upon UVB-irradiation, indicating a possible role of miR-124 in UVB-induced skin aging [121]. UCP2 is also associated with mir-26a-5p. Measured in serum, miR-26a could serve as a prognostic marker for osteoporosis and appears to regulate serum IGF1 levels in osteoporosis patients [122]. Additionally, mir-26a-5p has been linked with UVB-induced apoptosis [117]. Increased expression of miR-181a, which was predicted to be associated with WNT16, has been reported upregulated in keratinocytes undergoing replicative senescence [117]. Furthermore, miR-181a is among the biomarkers of aging expressed by dermal fibroblasts and has been linked with skin immunosenescence and the age-related inflammatory phenotype in CD4+ T cells [117].

While GO enrichment focuses on DEGs, a GSEA analysis takes the whole gene set into account. Thus, using NicheNet analysis, GSEA, the Omnipath database, and the well-known GSE113957 dataset, we present here to our knowledge the first integrated data analysis of the pathways involved in aging and progeria. Furthermore, we show genes and their interaction partners involved in these pathways.

According to our analysis, UV response has the highest positive normalized enrichment score when comparing nonagenarians and healthy children. Additionally, UV response is among the top five pathways when analyzing progeria. Lesiak et al. assessed the progerin expression upon sun exposure *in vivo* and demonstrated that one week of sun exposure was enough to significantly elevate the progerin levels in the skin of participants in their twenties almost to the amount of progerin measured in elderly participants (64.1 ±13.1 years) with photoaged skin [85]. Due to this experimentally backed correlation between UV exposure and progerin expression, we decided to focus on UV response in

 doi:10.20944/preprints202207.0038.v1

our NicheNet analyses. In both analyses, aging and progeria, IGF1 and CCL2 are among the prioritized ligands.

IGF1 (insulin-like growth factor 1) has been associated with IGFBP2 [112,123] and controls apoptosis [123,124]. Van den Beld and colleagues studied IGFBP2 and IGF1 concentrations, as well as insulin sensitivity and BMI in a 20-year longitudinal study and concluded that IGFBP2 levels can predict mortality if interpreted in relation to insulin sensitivity [112]. Hu et al. also reported a correlation between high IGFBP2 levels and mortality in subjects older than 70 years [123]. They proposed a possible association between low IGF1 expression, which is associated with lower mortality in animal models, and low IGFBP1 and IGFBP2 levels as markers for low IGF1 levels [123].

Fibroblasts of nonagenarians express less IGF1 than fibroblasts of healthy children, and IGF1 is indeed a DEG in natural aging. In fibroblasts donated by progeria patients, IGF1 appears to be slightly lower expressed than in nonagenarians. When comparing progeria patients and healthy children, IGF1 is also lower expressed.

As age appears to have a greater effect on UV-induced damages than the skin type [125], the effects of increased IGF1 expression were studied [126,127]. In aged skin, exogenous IGF1 [127] as well as dermabrasion and sun-protected skin-healing, which increased IGF1 levels [126], were found to restore the response to UVB radiation [126,127]. Therefore, it would be of interest whether treatments affecting IGF1 expression influence the progeria-related skin abnormalities.

Additionally, UV response might link inflammation and aging, “inflammaging”, as exposure to UV light is a well-known method to provoke inflammation [128], and CCL2 expression is also induced by inflammatory stimuli [129]. The C-C Motif Chemokine Ligand 2 (CCL2), which is also known under several other names, including monocyte chemoattractant protein-1 (MCP-1), is the other prioritized ligand aging and HGPS have in common when analyzed regarding UV response. Among its predicted interaction partners is ACKR4, the atypical chemokine receptor 4 that is also known as CCR11, and a variety of other names. ACKR4 is also among the CCL2-related DEGs that progeria and aging have in common. Although CCL2 levels are higher in progeria patients than in nonagenarians, both nonagenarians and progeria patients have higher CCL2 levels than healthy children.

Again, the individual facets are known, but the suggested synthesis sheds new light on this aging pathway. Since increased CCL2 levels have been associated with inflammation and aging, Luciano-Mateo and colleagues crossbred mice bearing a mutation in their LMNA gene with mice overexpressing CCL2 [130]. The combination of accelerated aging and CCL2 overexpression significantly reduced the lifespan and the health span of the mice [130]. Additionally, higher CCL2 levels appeared to worsen accelerated aging and also affected the energy metabolism and the 1-C metabolism, , as well as the mitochondrial function of the mice bearing both the LMNA mutation and CCL2 overexpression [130].

These results, as well as our observations, suggest CCL2 as an additional target in aging and progeria research. Therefore, we visualized the interactions of CCL2 and the CCL2-related DEGs involved in both aging and progeria. In this study, we focus on the interaction between CCL2 and ACKR4, as both are involved in the UV response pathway, which we selected as an example for NicheNet analysis. ACKR4 has been mentioned as a receptor for CCL2 [131] which is upregulated in nonagenarians compared to healthy children in our study, whereas the ACKR4 expression in progeria is very low in all comparisons. MCP-1/CCL2 can bind to a common binding site on ACKR4/CCR11 [131]. However, the relationship between CCL2 and ACKR4 is not yet explored. Hence, we predict that exploring the interactions of ACKR4 and CCL2 in aging in future research will be rather interesting.

Although we elaborated here only on UV response as an example, the other pathways suggested by NicheNet analysis are equally interesting, and focusing on the ligands and receptors involved might generate further insights regarding aging and progeria. Due to the plethora of information contained in RNA seq experiments, reanalyzing existing

RNA seq data can still generate new insights. Even if *in silico* analysis can offer great insights and help generate new hypotheses, subsequent *in vitro* and *in vivo* studies are necessary to further validate the targets found using omics analyses.

In summary, we briefly introduced several omics methods for RNA sequence analysis that can be used on their own or in combination with both new data and already existing publicly available data. Here, we introduced some of the differentially expressed genes, their interaction partners, and their age-related implications, hoping to demonstrate some of the possibilities omics analyses offer for aging research.

Supplementary Materials: The following supporting information can be downloaded at: www.mdpi.com/xxx/s1, Figure S1: CNET Plot of Enriched Hallmark Pathways when Comparing RNA Sequencing Data of HGPS Patients and Healthy Children; Figure S2: CNET Plot of Enriched Biological Processes when Comparing RNA Sequencing Data of HGPS Patients and Healthy Children; Figure S3: CNET Plot of Enriched Hallmark Pathways when Comparing RNA Sequencing Data of Nonagenarians and Healthy Children; Figure S4: CNET Plot of Enriched Biological Processes when Comparing RNA Sequencing Data of Nonagenarians and Healthy Children; Figure S5: Visualization of the DEGs involved in ECP using the log2foldchange Data of Comparing Nonagenarians and Healthy Children; Figure S6: miRNA Prediction and Network Visualization of miRNAs Related to WNT16 when Comparing Progeria Patients and Healthy Children; Figure S7: miRNA Prediction and Network Visualization of miRNAs Related to IGFBP2 when Comparing Progeria Patients and Healthy Children; Figure S8: miRNA Prediction and Network Visualization of miRNAs Related to UCP2 when Comparing Progeria Patients and Healthy Children; Table S1: Sample Information; Table S2: Overview Up- and Downregulated DEGs; Table S3: Gene Enrichment Biological Processes Analyses; Table S4: Predicted miRNAs; Document S1: Mini-Tutorial.

Author Contributions: Conceptualization, A.C., T.D. and S.D.; methodology, A.C.; formal analysis, A.C.; investigation, A.C.; resources, A.C. and T.D.; data curation, A.C.; writing—original draft preparation, A.C.; writing—review and editing, A.C., S.D., T.D., S.G. and S.A.W.C.; visualization, A.C.; supervision, T.D. and S.D.; project administration, T.D. and S.D.; funding acquisition, T.D. All authors have read and agreed to the published version of the manuscript.

Funding: This research was funded by Land of Bavaria, contribution to DFG-324392634–TRR221/INF [awarded to TD] and the APC was funded by University of Würzburg fund for open access publication.

Institutional Review Board Statement: Not applicable.

Informed Consent Statement: Not applicable.

Conflicts of Interest: The authors declare no conflict of interest.

References

1. López-Otín, C.; Blasco, M.A.; Partridge, L.; Serrano, M.; Kroemer, G. The Hallmarks of Aging. *Cell* **2013**, *153*, 1194-1217, doi:10.1016/j.cell.2013.05.039.
2. Hasin, Y.; Seldin, M.; Lusis, A. Multi-omics approaches to disease. *Genome Biology* **2017**, *18*, 83, doi:10.1186/s13059-017-1215-1.
3. ROYAL MEDICAL AND CHIRURGICAL SOCIETY. *The Lancet* **1886**, *127*, 922-923, doi:10.1016/S0140-6736(02)06582-0.
4. Keith, A. PROGERIA AND ATELEIOSIS. *The Lancet* **1913**, *181*, 305-313, doi:10.1016/S0140-6736(00)76131-9.
5. Gilford, H. PROGERIA AND ATELEIOSIS. *The Lancet* **1913**, *181*, 412-413, doi:10.1016/S0140-6736(01)20267-0.
6. Hegele, R.A. Drawing the line in progeria syndromes. *The Lancet* **2003**, *362*, 416-417, doi:10.1016/S0140-6736(03)14097-4.
7. Merideth, M.A.; Gordon, L.B.; Clauss, S.; Sachdev, V.; Smith, A.C.M.; Perry, M.B.; Brewer, C.C.; Zalewski, C.; Kim, H.J.; Solomon, B.; et al. Phenotype and Course of Hutchinson–Gilford Progeria Syndrome. *New England Journal of Medicine* **2008**, *358*, 592-604, doi:10.1056/NEJMoa0706898.
8. Hennekam, R.C.M. Hutchinson–Gilford progeria syndrome: Review of the phenotype. *American Journal of Medical Genetics Part A* **2006**, *140A*, 2603-2624, doi:https://doi.org/10.1002/ajmg.a.31346.
9. Eriksson, M.; Brown, W.T.; Gordon, L.B.; Glynn, M.W.; Singer, J.; Scott, L.; Erdos, M.R.; Robbins, C.M.; Moses, T.Y.; Berglund, P.; et al. Recurrent de novo point mutations in lamin A cause Hutchinson–Gilford progeria syndrome. *Nature* **2003**, *423*, 293-298, doi:10.1038/nature01629.

10. Osmanagic-Myers, S.; Kiss, A.; Manakanatas, C.; Hamza, O.; Sedlmayer, F.; Szabo, P.L.; Fischer, I.; Fichtinger, P.; Podesser, B.K.; Eriksson, M.; et al. Endothelial progerin expression causes cardiovascular pathology through an impaired mechanoresponse. *The Journal of Clinical Investigation* **2019**, *129*, 531-545, doi:10.1172/JCI121297.
11. De Sandre-Giovannoli, A.; Bernard, R.; Cau, P.; Navarro, C.; Amiel, J.; Boccaccio, I.; Lyonnet, S.; Stewart Colin, L.; Munnich, A.; Le Merrer, M.; et al. Lamin A Truncation in Hutchinson-Gilford Progeria. *Science* **2003**, *300*, 2055-2055, doi:10.1126/science.1084125.
12. Gordon Leslie, B.; Kleinman Monica, E.; Miller David, T.; Neuberg Donna, S.; Giobbie-Hurder, A.; Gerhard-Herman, M.; Smoot Leslie, B.; Gordon Catherine, M.; Cleveland, R.; Snyder Brian, D.; et al. Clinical trial of a farnesyltransferase inhibitor in children with Hutchinson–Gilford progeria syndrome. *Proceedings of the National Academy of Sciences* **2012**, *109*, 16666-16671, doi:10.1073/pnas.1202529109.
13. Gordon, L.B.; Kleinman, M.E.; Massaro, J.; D'Agostino, R.B.; Shappell, H.; Gerhard-Herman, M.; Smoot, L.B.; Gordon, C.M.; Cleveland, R.H.; Nazarian, A.; et al. Clinical Trial of the Protein Farnesylation Inhibitors Lonafarnib, Pravastatin, and Zoledronic Acid in Children With Hutchinson-Gilford Progeria Syndrome. *Circulation* **2016**, *134*, 114-125, doi:10.1161/CIRCULATIONAHA.116.022188.
14. Dhillon, S. Lonafarnib: First Approval. *Drugs* **2021**, *81*, 283-289, doi:10.1007/s40265-020-01464-z.
15. The Progeria Research Foundation. News - European Medicines Agency recommends Zokinvy, the first and only therapy to treat ultra-rare, rapid-ageing disease progeria, for approval in Europe. Available online: https://www.progeriaresearch.org/ (accessed on
16. Fleischer, J.G.; Schulte, R.; Tsai, H.H.; Tyagi, S.; Ibarra, A.; Shokhirev, M.N.; Huang, L.; Hetzer, M.W.; Navlakha, S. Predicting age from the transcriptome of human dermal fibroblasts. *Genome Biology* **2018**, *19*, 221, doi:10.1186/s13059-018-1599-6.
17. Fleischer JG, S.R., Tsai H, Tyagi S, Ibarra A, Shokhirev MN, Huang L, Hetzer MW, Navlakha S. Predicting age from the transcriptome of human dermal fibroblasts. **2018**.
18. Edgar, R.; Domrachev, M.; Lash, A.E. Gene Expression Omnibus: NCBI gene expression and hybridization array data repository. *Nucleic Acids Research* **2002**, *30*, 207-210, doi:10.1093/nar/30.1.207.
19. Kramme, C.; Plesa, A.M.; Wang, H.H.; Wolf, B.; Smela, M.P.; Guo, X.; Kohman, R.E.; Chatterjee, P.; Church, G.M. An integrated pipeline for mammalian genetic screening. *Cell Reports Methods* **2021**, *1*, 100082, doi:https://doi.org/10.1016/j.crmeth.2021.100082.
20. Ikegami, K.; Secchia, S.; Almakki, O.; Lieb, J.D.; Moskowitz, I.P. Phosphorylated Lamin A/C in the Nuclear Interior Binds Active Enhancers Associated with Abnormal Transcription in Progeria. *Developmental Cell* **2020**, *52*, 699-713.e611, doi:10.1016/j.devcel.2020.02.011.
21. Roth, S.H.; Levanon, E.Y.; Eisenberg, E. Genome-wide quantification of ADAR adenosine-to-inosine RNA editing activity. *Nature Methods* **2019**, *16*, 1131-1138, doi:10.1038/s41592-019-0610-9.
22. Lee, Y.; Shivashankar, G.V. Analysis of transcriptional modules during human fibroblast ageing. *Scientific Reports* **2020**, *10*, 19086, doi:10.1038/s41598-020-76117-y.
23. LaRocca, T.J.; Cavalier, A.N.; Wahl, D. Repetitive elements as a transcriptomic marker of aging: Evidence in multiple datasets and models. *Aging Cell* **2020**, *19*, e13167, doi:https://doi.org/10.1111/acel.13167.
24. Yao, J.; Ding, D.; Li, X.; Shen, T.; Fu, H.; Zhong, H.; Wei, G.; Ni, T. Prevalent intron retention fine-tunes gene expression and contributes to cellular senescence. *Aging Cell* **2020**, *19*, e13276, doi:https://doi.org/10.1111/acel.13276.
25. Köhler, F.; Bormann, F.; Raddatz, G.; Gutekunst, J.; Corless, S.; Musch, T.; Lonsdorf, A.S.; Erhardt, S.; Lyko, F.; Rodríguez-Paredes, M. Epigenetic deregulation of lamina-associated domains in Hutchinson-Gilford progeria syndrome. *Genome Medicine* **2020**, *12*, 46, doi:10.1186/s13073-020-00749-y.
26. Bickler, S.W.; Cauvi, D.M.; Fisch, K.M.; Prieto, J.M.; Sykes, A.G.; Thangarajah, H.; Lazar, D.A.; Ignacio, R.C.; Gerstmann, D.R.; Ryan, A.F.; et al. Extremes of age are associated with differences in the expression of selected pattern recognition receptor genes and ACE2, the receptor for SARS-CoV-2: implications for the epidemiology of COVID-19 disease. *BMC Medical Genomics* **2021**, *14*, 138, doi:10.1186/s12920-021-00970-7.
27. Gill, D.; Parry, A.; Santos, F.; Okkenhaug, H.; Todd, C.D.; Hernando-Herraez, I.; Stubbs, T.M.; Milagre, I.; Reik, W. Multi-omic rejuvenation of human cells by maturation phase transient reprogramming. *eLife* **2022**, *11*, e71624, doi:10.7554/eLife.71624.
28. McCauley, B.S.; Sun, L.; Yu, R.; Lee, M.; Liu, H.; Leeman, D.S.; Huang, Y.; Webb, A.E.; Dang, W. Altered chromatin states drive cryptic transcription in aging mammalian stem cells. *Nature Aging* **2021**, *1*, 684-697, doi:10.1038/s43587-021-00091-x.
29. Meyer, D.H.; Schumacher, B. BiT age: A transcriptome-based aging clock near the theoretical limit of accuracy. *Aging Cell* **2021**, *20*, e13320, doi:https://doi.org/10.1111/acel.13320.
30. Yim, A.; Koti, P.; Bonnard, A.; Marchiano, F.; Dürrbaum, M.; Garcia-Perez, C.; Villaveces, J.; Gamal, S.; Cardone, G.; Perocchi, F.; et al. mitoXplorer, a visual data mining platform to systematically analyze and visualize mitochondrial expression dynamics and mutations. *Nucleic Acids Research* **2020**, *48*, 605-632, doi:10.1093/nar/gkz1128.
31. Gabay, O.; Shoshan, Y.; Kopel, E.; Ben-Zvi, U.; Mann, T.D.; Bressler, N.; Cohen-Fultheim, R.; Schaffer, A.A.; Roth, S.H.; Tzur, Z.; et al. Landscape of adenosine-to-inosine RNA recoding across human tissues. *Nature Communications* **2022**, *13*, 1184, doi:10.1038/s41467-022-28841-4.
32. R Core Team. R: A Language and Environment for Statistical Computing. **2021**.
33. Barrett, T.; Wilhite, S.E.; Ledoux, P.; Evangelista, C.; Kim, I.F.; Tomashevsky, M.; Marshall, K.A.; Phillippy, K.H.; Sherman, P.M.; Holko, M.; et al. NCBI GEO: archive for functional genomics data sets—update. *Nucleic Acids Research* **2013**, *41*, D991-D995, doi:10.1093/nar/gks1193.

34. Andrews, S. FastQC: A Quality Control Tool for High Throughput Sequence Data [Online]. Available online at: http://www.bioinformatics.babraham.ac.uk/projects/fastqc/. **2010**.
35. Ewels, P.; Magnusson, M.; Lundin, S.; Käller, M. MultiQC: summarize analysis results for multiple tools and samples in a single report. *Bioinformatics* **2016**, *32*, 3047-3048, doi:10.1093/bioinformatics/btw354.
36. Frankish, A.; Diekhans, M.; Ferreira, A.-M.; Johnson, R.; Jungreis, I.; Loveland, J.; Mudge, J.M.; Sisu, C.; Wright, J.; Armstrong, J.; et al. GENCODE reference annotation for the human and mouse genomes. *Nucleic Acids Research* **2019**, *47*, D766-D773, doi:10.1093/nar/gky955.
37. Dobin, A.; Davis, C.A.; Schlesinger, F.; Drenkow, J.; Zaleski, C.; Jha, S.; Batut, P.; Chaisson, M.; Gingeras, T.R. STAR: ultrafast universal RNA-seq aligner. *Bioinformatics* **2013**, *29*, 15-21, doi:10.1093/bioinformatics/bts635.
38. Li, B.; Dewey, C.N. RSEM: accurate transcript quantification from RNA-Seq data with or without a reference genome. *BMC Bioinformatics* **2011**, *12*, 323, doi:10.1186/1471-2105-12-323.
39. Love, M.I.; Huber, W.; Anders, S. Moderated estimation of fold change and dispersion for RNA-seq data with DESeq2. *Genome Biology* **2014**, *15*, 550, doi:10.1186/s13059-014-0550-8.
40. Zhu, A.; Ibrahim, J.G.; Love, M.I. Heavy-tailed prior distributions for sequence count data: removing the noise and preserving large differences. *Bioinformatics* **2019**, *35*, 2084-2092, doi:10.1093/bioinformatics/bty895.
41. Soneson, C.; Love, M.; Robinson, M. Differential analyses for RNA-seq: transcript-level estimates improve gene-level inferences [version 2; peer review: 2 approved]. *F1000Research* **2016**, *4*, doi:10.12688/f1000research.7563.2.
42. Blighe, K.; Rana, S.; Lewis, M. EnhancedVolcano: Publication-ready volcano plots with enhanced colouring and labeling. **2022**.
43. Kolde, R. pheatmap: Pretty Heatmaps. R package version 1.0.12. https://CRAN.R-project.org/package=pheatmap. **2019**.
44. Vitting-Seerup, K.; Sandelin, A. The Landscape of Isoform Switches in Human Cancers. *Molecular Cancer Research* **2017**, *15*, 1206-1220, doi:10.1158/1541-7786.MCR-16-0459.
45. Subramanian, A.; Tamayo, P.; Mootha Vamsi, K.; Mukherjee, S.; Ebert Benjamin, L.; Gillette Michael, A.; Paulovich, A.; Pomeroy Scott, L.; Golub Todd, R.; Lander Eric, S.; et al. Gene set enrichment analysis: A knowledge-based approach for interpreting genome-wide expression profiles. *Proceedings of the National Academy of Sciences* **2005**, *102*, 15545-15550, doi:10.1073/pnas.0506580102.
46. Liberzon, A.; Birger, C.; Thorvaldsdóttir, H.; Ghandi, M.; Mesirov, J.P.; Tamayo, P. The Molecular Signatures Database (MSigDB) hallmark gene set collection. *Cell systems* **2015**, *1*, 417-425, doi:10.1016/j.cels.2015.12.004.
47. Ashburner, M.; Ball, C.A.; Blake, J.A.; Botstein, D.; Butler, H.; Cherry, J.M.; Davis, A.P.; Dolinski, K.; Dwight, S.S.; Eppig, J.T.; et al. Gene Ontology: tool for the unification of biology. *Nature Genetics* **2000**, *25*, 25-29, doi:10.1038/75556.
48. The Gene Ontology, C. The Gene Ontology resource: enriching a GOld mine. *Nucleic Acids Research* **2021**, *49*, D325-D334, doi:10.1093/nar/gkaa1113.
49. Yu, G.; Wang, L.-G.; Han, Y.; He, Q.-Y. clusterProfiler: an R Package for Comparing Biological Themes Among Gene Clusters. *OMICS: A Journal of Integrative Biology* **2012**, *16*, 284-287, doi:10.1089/omi.2011.0118.
50. Wang, H.; Chen, X.; Bao, L.; Zhang, X. Investigating potential molecular mechanisms of serum exosomal miRNAs in colorectal cancer based on bioinformatics analysis. *Medicine* **2020**, *99*.
51. Chagoyen, M.; Pazos, F. Quantifying the biological significance of gene ontology biological processes—implications for the analysis of systems-wide data. *Bioinformatics* **2010**, *26*, 378-384, doi:10.1093/bioinformatics/btp663.
52. Wu, T.; Hu, E.; Xu, S.; Chen, M.; Guo, P.; Dai, Z.; Feng, T.; Zhou, L.; Tang, W.; Zhan, L.; et al. clusterProfiler 4.0: A universal enrichment tool for interpreting omics data. *The Innovation* **2021**, *2*, doi:10.1016/j.xinn.2021.100141.
53. Yu, G. *enrichplot: Visualization of Functional Enrichment Result*, 2022.
54. Wickham, H. *ggplot2: Elegant Graphics for Data Analysis*; Springer-Verlag New York: 2016.
55. Szklarczyk, D.; Gable, A.L.; Lyon, D.; Junge, A.; Wyder, S.; Huerta-Cepas, J.; Simonovic, M.; Doncheva, N.T.; Morris, J.H.; Bork, P.; et al. STRING v11: protein–protein association networks with increased coverage, supporting functional discovery in genome-wide experimental datasets. *Nucleic Acids Research* **2019**, *47*, D607-D613, doi:10.1093/nar/gky1131.
56. Jensen, L.J.; Kuhn, M.; Stark, M.; Chaffron, S.; Creevey, C.; Muller, J.; Doerks, T.; Julien, P.; Roth, A.; Simonovic, M.; et al. STRING 8—a global view on proteins and their functional interactions in 630 organisms. *Nucleic Acids Research* **2009**, *37*, D412-D416, doi:10.1093/nar/gkn760.
57. Shannon, P.; Markiel, A.; Ozier, O.; Baliga, N.S.; Wang, J.T.; Ramage, D.; Amin, N.; Schwikowski, B.; Ideker, T. Cytoscape: A Software Environment for Integrated Models of Biomolecular Interaction Networks. *Genome Research* **2003**, *13*, 2498-2504, doi:10.1101/gr.1239303.
58. Venn, J. I. On the diagrammatic and mechanical representation of propositions and reasonings. *The London, Edinburgh, and Dublin Philosophical Magazine and Journal of Science* **1880**, *10*, 1-18, doi:10.1080/14786448008626877.
59. Oliveros, J.C. Venny. An interactive tool for comparing lists with Venn's diagrams. Access at: https://bioinfogp.cnb.csic.es/tools/venny/index.html. **2007-2015**.
60. Chang, L.; Zhou, G.; Soufan, O.; Xia, J. miRNet 2.0: network-based visual analytics for miRNA functional analysis and systems biology. *Nucleic Acids Research* **2020**, *48*, W244-W251, doi:10.1093/nar/gkaa467.
61. Türei, D.; Valdeolivas, A.; Gul, L.; Palacio-Escat, N.; Klein, M.; Ivanova, O.; Ölbei, M.; Gábor, A.; Theis, F.; Módos, D.; et al. Integrated intra- and intercellular signaling knowledge for multicellular omics analysis. *Molecular Systems Biology* **2021**, *17*, e9923, doi:https://doi.org/10.15252/msb.20209923.

62. Browaeys, R.; Saelens, W.; Saeys, Y. NicheNet: modeling intercellular communication by linking ligands to target genes. *Nature Methods* **2020**, *17*, 159-162, doi:10.1038/s41592-019-0667-5.
63. Korotkevich, G.; Sukhov, V.; Budin, N.; Shpak, B.; Artyomov, M.N.; Sergushichev, A. Fast gene set enrichment analysis. *bioRxiv* **2021**, 060012, doi:10.1101/060012.
64. Wilke, C.O. cowplot: Streamlined Plot Theme and Plot Annotations for 'ggplot2'. **2020**.
65. Yu, G. ggplotify: Convert Plot to 'grob' or 'ggplot' Object. **2021**.
66. Ooms, J. magick: Advanced Graphics and Image-Processing in R. **2021**.
67. Ligges, U.; Maechler, M. scatterplot3d - An R Package for Visualizing Multivariate Data. *Journal of Statistical Software* **2003**, *8*, 1 - 20, doi:10.18637/jss.v008.i11.
68. Wickham, H.; Seidel, D. scales: Scale Functions for Visualization. **2022**.
69. Garnier, S.; Ross, N.; Rudis, R.; Camargo, A.P.; Sciaini, M.; Scherer, C. Rvision - Colorblind-Friendly Color Maps for R. **2021**, doi:10.5281/zenodo.4679424.
70. Sievert, C. *Interactive Web-Based Data Visualization with R, plotly, and shiny*; Chapman and Hall/CRC: 2020.
71. Neuwirth, E. RColorBrewer: ColorBrewer Palettes. **2022**.
72. Ahlmann-Eltze, C. ggupset: Combination Matrix Axis for 'ggplot2' to Create 'UpSet' Plots. **2020**.
73. Campitelli, E. ggnewscale: Multiple Fill and Colour Scales in 'ggplot2'. **2022**.
74. Luo, W.; Brouwer, C. Pathview: an R/Bioconductor package for pathway-based data integration and visualization. *Bioinformatics* **2013**, *29*, 1830-1831, doi:10.1093/bioinformatics/btt285.
75. Wilke, C.O. ggridges: Ridgeline Plots in 'ggplot2'. **2021**.
76. Jahn, N. europepmc: R Interface to the Europe PubMed Central RESTful Web Service. **2021**.
77. Morgan, M. BiocManager: Access the Bioconductor Project Package Repository. **2022**.
78. Carlson, M. org.Hs.eg.db: Genome wide annotation for Human. **2022**.
79. Wickham, H.; Averick, M.; Bryan, J.; Chang, W.; McGowan, L.; François, R.; Grolemund, G.; Hayes, A.; Henry, L.; Hester, J.; et al. Welcome to the Tidyverse. *Journal of Open Source Software* **2019**, *4*, 1686, doi:10.21105/joss.01686.
80. Wickham, H.; François, R.; Henry, L.; Müller, K. dplyr: A Grammar of Data Manipulation. **2022**.
81. Gordon, L.B.; Brown, W.T.; Collins, F.S. Hutchinson-Gilford Progeria Syndrome. In *GeneReviews(®)*, Adam, M.P., Ardinger, H.H., Pagon, R.A., Wallace, S.E., Bean, L.J.H., Gripp, K.W., Mirzaa, G.M., Amemiya, A., Eds.; University of Washington, Seattle
Copyright © 1993-2022, University of Washington, Seattle. GeneReviews is a registered trademark of the University of Washington, Seattle. All rights reserved.: Seattle (WA), 1993-2022.
82. Liberzon, A.; Birger, C.; Thorvaldsdóttir, H.; Ghandi, M.; Mesirov, Jill P.; Tamayo, P. The Molecular Signatures Database Hallmark Gene Set Collection. *Cell Systems* **2015**, *1*, 417-425, doi:10.1016/j.cels.2015.12.004.
83. Dangwal, S.; Thum, T. microRNA Therapeutics in Cardiovascular Disease Models. *Annual Review of Pharmacology and Toxicology* **2014**, *54*, 185-203, doi:10.1146/annurev-pharmtox-011613-135957.
84. Türei, D.; Korcsmáros, T.; Saez-Rodriguez, J. OmniPath: guidelines and gateway for literature-curated signaling pathway resources. *Nature Methods* **2016**, *13*, 966-967, doi:10.1038/nmeth.4077.
85. Lesiak, A.; Bednarski, I.; Rogowski-Tylman, M.; Sobjanek, M.; Woźniacka, A.; Danilewicz, M.; Young, A.; Narbutt, J. One week of exposure to sunlight induces progerin expression in human skin. *Advances in Dermatology and Allergology/Postępy Dermatologii i Alergologii* **2017**, *34*, 629-631, doi:10.5114/pdia.2016.62416.
86. McClintock, D.; Gordon Leslie, B.; Djabali, K. Hutchinson–Gilford progeria mutant lamin A primarily targets human vascular cells as detected by an anti-Lamin A G608G antibody. *Proceedings of the National Academy of Sciences* **2006**, *103*, 2154-2159, doi:10.1073/pnas.0511133103.
87. Olive, M.; Harten, I.; Mitchell, R.; Beers, J.K.; Djabali, K.; Cao, K.; Erdos, M.R.; Blair, C.; Funke, B.; Smoot, L.; et al. Cardiovascular Pathology in Hutchinson-Gilford Progeria: Correlation With the Vascular Pathology of Aging. *Arteriosclerosis, Thrombosis, and Vascular Biology* **2010**, *30*, 2301-2309, doi:10.1161/ATVBAHA.110.209460.
88. Rowe John, W.; Kahn Robert, L. Human Aging: Usual and Successful. *Science* **1987**, *237*, 143-149, doi:10.1126/science.3299702.
89. Franceschi, C.; Garagnani, P.; Morsiani, C.; Conte, M.; Santoro, A.; Grignolio, A.; Monti, D.; Capri, M.; Salvioli, S. The Continuum of Aging and Age-Related Diseases: Common Mechanisms but Different Rates. *Frontiers in Medicine* **2018**, *5*, doi:10.3389/fmed.2018.00061.
90. Fulop, T.; Larbi, A.; Khalil, A.; Cohen, A.A.; Witkowski, J.M. Are We Ill Because We Age? *Frontiers in Physiology* **2019**, *10*, doi:10.3389/fphys.2019.01508.
91. Gordon, L.B.; Shappell, H.; Massaro, J.; D'Agostino, R.B., Sr; Brazier, J.; Campbell, S.E.; Kleinman, M.E.; Kieran, M.W. Association of Lonafarnib Treatment vs No Treatment With Mortality Rate in Patients With Hutchinson-Gilford Progeria Syndrome. *JAMA* **2018**, *319*, 1687-1695, doi:10.1001/jama.2018.3264.
92. Berndt, N.; Hamilton, A.D.; Sebti, S.M. Targeting protein prenylation for cancer therapy. *Nat Rev Cancer* **2011**, *11*, 775-791, doi:10.1038/nrc3151.
93. Xie, C.; Li, Y.; Li, L.-L.; Fan, X.-X.; Wang, Y.-W.; Wei, C.-L.; Liu, L.; Leung, E.L.-H.; Yao, X.-J. Identification of a New Potent Inhibitor Targeting KRAS in Non-small Cell Lung Cancer Cells. *Front Pharmacol* **2017**, *8*, 823-823, doi:10.3389/fphar.2017.00823.
94. Macicior, J.; Marcos-Ramiro, B.; Ortega-Gutiérrez, S. Small-Molecule Therapeutic Perspectives for the Treatment of Progeria. *International Journal of Molecular Sciences* **2021**, *22*, 7190.

95. Schurch, N.J.; Schofield, P.; Gierliński, M.; Cole, C.; Sherstnev, A.; Singh, V.; Wrobel, N.; Gharbi, K.; Simpson, G.G.; Owen-Hughes, T.; et al. How many biological replicates are needed in an RNA-seq experiment and which differential expression tool should you use? *Rna* **2016**, *22*, 839-851, doi:10.1261/rna.053959.115.
96. Schurch, N.J.; Schofield, P.; Gierliński, M.; Cole, C.; Sherstnev, A.; Singh, V.; Wrobel, N.; Gharbi, K.; Simpson, G.G.; Owen-Hughes, T.; et al. Erratum: How many biological replicates are needed in an RNA-seq experiment and which differential expression tool should you use? *Rna* **2016**, *22*, 1641, doi:10.1261/rna.058339.116.
97. Miao, Q.; Xu, Y.; Yin, H.; Zhang, H.; Ye, J. KRT8 phosphorylation regulates the epithelial-mesenchymal transition in retinal pigment epithelial cells through autophagy modulation. *Journal of Cellular and Molecular Medicine* **2020**, *24*, 3217-3228, doi:https://doi.org/10.1111/jcmm.14998.
98. Cardoso, A.L.; Fernandes, A.; Aguilar-Pimentel, J.A.; de Angelis, M.H.; Guedes, J.R.; Brito, M.A.; Ortolano, S.; Pani, G.; Athanasopoulou, S.; Gonos, E.S.; et al. Towards frailty biomarkers: Candidates from genes and pathways regulated in aging and age-related diseases. *Ageing Research Reviews* **2018**, *47*, 214-277, doi:https://doi.org/10.1016/j.arr.2018.07.004.
99. Kelwick, R.; Desanlis, I.; Wheeler, G.N.; Edwards, D.R. The ADAMTS (A Disintegrin and Metalloproteinase with Thrombospondin motifs) family. *Genome Biology* **2015**, *16*, 113, doi:10.1186/s13059-015-0676-3.
100. Talpin, A.; Costantino, F.; Bonilla, N.; Leboime, A.; Letourneur, F.; Jacques, S.; Dumont, F.; Amraoui, S.; Dutertre, C.-A.; Garchon, H.-J.; et al. Monocyte-derived dendritic cells from HLA-B27+ axial spondyloarthritis (SpA) patients display altered functional capacity and deregulated gene expression. *Arthritis Research & Therapy* **2014**, *16*, 417, doi:10.1186/s13075-014-0417-0.
101. Cheetham, S.W.; Faulkner, G.J.; Dinger, M.E. Overcoming challenges and dogmas to understand the functions of pseudogenes. *Nature Reviews Genetics* **2020**, *21*, 191-201, doi:10.1038/s41576-019-0196-1.
102. Pink, R.C.; Wicks, K.; Caley, D.P.; Punch, E.K.; Jacobs, L.; Carter, D.R.F. Pseudogenes: pseudo-functional or key regulators in health and disease? *RNA (New York, N.Y.)* **2011**, *17*, 792-798, doi:10.1261/rna.2658311.
103. Kovalenko, T.F.; Patrushev, L.I. Pseudogenes as Functionally Significant Elements of the Genome. *Biochemistry (Moscow)* **2018**, *83*, 1332-1349, doi:10.1134/S0006297918110044.
104. Marthandan, S.; Baumgart, M.; Priebe, S.; Groth, M.; Schaer, J.; Kaether, C.; Guthke, R.; Cellerino, A.; Platzer, M.; Diekmann, S.; et al. Conserved Senescence Associated Genes and Pathways in Primary Human Fibroblasts Detected by RNA-Seq. *PLOS ONE* **2016**, *11*, e0154531, doi:10.1371/journal.pone.0154531.
105. Todd, H.; Galea, G.L.; Meakin, L.B.; Delisser, P.J.; Lanyon, L.E.; Windahl, S.H.; Price, J.S. Wnt16 Is Associated with Age-Related Bone Loss and Estrogen Withdrawal in Murine Bone. *PLOS ONE* **2015**, *10*, e0140260, doi:10.1371/journal.pone.0140260.
106. Binet, R.; Ythier, D.; Robles, A.I.; Collado, M.; Larrieu, D.; Fonti, C.; Brambilla, E.; Brambilla, C.; Serrano, M.; Harris, C.C.; et al. WNT16B Is a New Marker of Cellular Senescence That Regulates p53 Activity and the Phosphoinositide 3-Kinase/AKT Pathway. *Cancer Research* **2009**, *69*, 9183-9191, doi:10.1158/0008-5472.Can-09-1016.
107. Sola-Carvajal, A.; Revêchon, G.; Helgadottir, H.T.; Whisenant, D.; Hagblom, R.; Döhla, J.; Katajisto, P.; Brodin, D.; Fagerström-Billai, F.; Viceconte, N.; et al. Accumulation of Progerin Affects the Symmetry of Cell Division and Is Associated with Impaired Wnt Signaling and the Mislocalization of Nuclear Envelope Proteins. *Journal of Investigative Dermatology* **2019**, *139*, 2272-2280.e2212, doi:https://doi.org/10.1016/j.jid.2019.05.005.
108. Hirose, M.; Schilf, P.; Lange, F.; Mayer, J.; Reichart, G.; Maity, P.; Jöhren, O.; Schwaninger, M.; Scharffetter-Kochanek, K.; Sina, C.; et al. Uncoupling protein 2 protects mice from aging. *Mitochondrion* **2016**, *30*, 42-50, doi:https://doi.org/10.1016/j.mito.2016.06.004.
109. Tian, X.Y.; Ma, S.; Tse, G.; Wong, W.T.; Huang, Y. Uncoupling Protein 2 in Cardiovascular Health and Disease. *Frontiers in Physiology* **2018**, *9*, doi:10.3389/fphys.2018.01060.
110. Kukat, A.; Dogan, S.A.; Edgar, D.; Mourier, A.; Jacoby, C.; Maiti, P.; Mauer, J.; Becker, C.; Senft, K.; Wibom, R.; et al. Loss of UCP2 Attenuates Mitochondrial Dysfunction without Altering ROS Production and Uncoupling Activity. *PLOS Genetics* **2014**, *10*, e1004385, doi:10.1371/journal.pgen.1004385.
111. Lopez-Mejia, I.C.; de Toledo, M.; Chavey, C.; Lapasset, L.; Cavelier, P.; Lopez-Herrera, C.; Chebli, K.; Fort, P.; Beranger, G.; Fajas, L.; et al. Antagonistic functions of LMNA isoforms in energy expenditure and lifespan. *EMBO reports* **2014**, *15*, 529-539, doi:https://doi.org/10.1002/embr.201338126.
112. van den Beld, A.; Carlson, O.; Doyle, M.E.; Rizopoulos, D.; Ferrucci, L.; Van der Lely, A.J.; Egan, J. IGFBP-2 And Aging; A 20 Year Longitudinal Study on IGFBP-2, IGF-I, BMI, Insulin Sensitivity and Mortality in an Aging Population. *European Journal of Endocrinology* **2018**, EJE-18-0422, doi:10.1530/EJE-18-0422.
113. Sisu, C. Pseudogenes as Biomarkers and Therapeutic Targets in Human Cancers. *Methods Mol Biol* **2021**, *2324*, 319-337, doi:10.1007/978-1-0716-1503-4_20.
114. Salmena, L. Pseudogenes: Four Decades of Discovery. *Methods Mol Biol* **2021**, *2324*, 3-18, doi:10.1007/978-1-0716-1503-4_1.
115. Dangwal, S.; Schimmel, K.; Foinquinos, A.; Xiao, K.; Thum, T. Noncoding RNAs in Heart Failure. In *Heart Failure*, Bauersachs, J., Butler, J., Sandner, P., Eds.; Springer International Publishing: Cham, 2017; pp. 423-445.
116. Hinkel, R.; Batkai, S.; Bähr, A.; Bozoglu, T.; Straub, S.; Borchert, T.; Viereck, J.; Howe, A.; Hornaschewitz, N.; Oberberger, L.; et al. AntimiR-132 Attenuates Myocardial Hypertrophy in an Animal Model of Percutaneous Aortic Constriction. *Journal of the American College of Cardiology* **2021**, *77*, 2923-2935, doi:https://doi.org/10.1016/j.jacc.2021.04.028.
117. Gerasymchuk, M.; Cherkasova, V.; Kovalchuk, O.; Kovalchuk, I. The Role of microRNAs in Organismal and Skin Aging. *International Journal of Molecular Sciences* **2020**, *21*, 5281.

118. ElSharawy, A.; Keller, A.; Flachsbart, F.; Wendschlag, A.; Jacobs, G.; Kefer, N.; Brefort, T.; Leidinger, P.; Backes, C.; Meese, E.; et al. Genome-wide miRNA signatures of human longevity. *Aging Cell* **2012**, *11*, 607-616, doi:https://doi.org/10.1111/j.1474-9726.2012.00824.x.
119. Olivieri, F.; Bonafè, M.; Spazzafumo, L.; Gobbi, M.; Prattichizzo, F.; Recchioni, R.; Marcheselli, F.; La Sala, L.; Galeazzi, R.; Rippo, M.R.; et al. Age- and glycemia-related miR-126-3p levels in plasma and endothelial cells. *Aging (Albany NY)* **2014**, *6*, 771-787, doi:10.18632/aging.100693.
120. Bi, Q.; Liu, J.; Wang, X.; Sun, F. Downregulation of miR-27b promotes skin wound healing in a rat model of scald burn by promoting fibroblast proliferation. *Exp Ther Med* **2020**, *20*, 63-63, doi:10.3892/etm.2020.9191.
121. Harada, M.; Jinnin, M.; Wang, Z.; Hirano, A.; Tomizawa, Y.; Kira, T.; Igata, T.; Masuguchi, S.; Fukushima, S.; Ihn, H. The expression of miR-124 increases in aged skin to cause cell senescence and it decreases in squamous cell carcinoma. *BioScience Trends* **2016**, *10*, 454-459, doi:10.5582/bst.2016.01102.
122. Yuan, F.; Chen, H.; Hu, P.; Su, P.; Guan, X. MiR-26a regulates the expression of serum IGF-1 in patients with osteoporosis and its effect on proliferation and apoptosis of mouse chondrocytes. *J Musculoskelet Neuronal Interact* **2021**, *21*, 298-307.
123. Hu, D.; Pawlikowska, L.; Kanaya, A.; Hsueh, W.-C.; Colbert, L.; Newman, A.B.; Satterfield, S.; Rosen, C.; Cummings, S.R.; Harris, T.B.; et al. Serum Insulin-Like Growth Factor-1 Binding Proteins 1 and 2 and Mortality in Older Adults: The Health, Aging, and Body Composition Study. *Journal of the American Geriatrics Society* **2009**, *57*, 1213-1218, doi:https://doi.org/10.1111/j.1532-5415.2009.02318.x.
124. Kooijman, R. Regulation of apoptosis by insulin-like growth factor (IGF)-I. *Cytokine & Growth Factor Reviews* **2006**, *17*, 305-323, doi:https://doi.org/10.1016/j.cytogfr.2006.02.002.
125. Kemp, M.G.; Spandau, D.F.; Travers, J.B. Impact of Age and Insulin-Like Growth Factor-1 on DNA Damage Responses in UV-Irradiated Human Skin. *Molecules* **2017**, *22*, doi:10.3390/molecules22030356.
126. Lewis, D.A.; Travers, J.B.; Machado, C.; Somani, A.-K.; Spandau, D.F. Reversing the aging stromal phenotype prevents carcinoma initiation. *Aging* **2011**, *3*, 407-416, doi:10.18632/aging.100318.
127. Lewis, D.A.; Travers, J.B.; Somani, A.K.; Spandau, D.F. The IGF-1/IGF-1R signaling axis in the skin: a new role for the dermis in aging-associated skin cancer. *Oncogene* **2010**, *29*, 1475-1485, doi:10.1038/onc.2009.440.
128. Hruza, L.L.; Pentland, A.P. Mechanisms of UV-induced inflammation. *J Invest Dermatol* **1993**, *100*, 35s-41s, doi:10.1111/1523-1747.ep12355240.
129. Gschwandtner, M.; Derler, R.; Midwood, K.S. More Than Just Attractive: How CCL2 Influences Myeloid Cell Behavior Beyond Chemotaxis. *Frontiers in Immunology* **2019**, *10*, doi:10.3389/fimmu.2019.02759.
130. Luciano-Mateo, F.; Cabré, N.; Baiges-Gaya, G.; Fernández-Arroyo, S.; Hernández-Aguilera, A.; Elisabet Rodríguez-Tomàs, E.; Arenas, M.; Camps, J.; Menéndez, J.A.; Joven, J. Systemic overexpression of C-C motif chemokine ligand 2 promotes metabolic dysregulation and premature death in mice with accelerated aging. *Aging* **2020**, *12*, 20001-20023, doi:10.18632/aging.104154.
131. Schweickart, V.L.; Epp, A.; Raport, C.J.; Gray, P.W. CCR11 Is a Functional Receptor for the Monocyte Chemoattractant Protein Family of Chemokines *. *Journal of Biological Chemistry* **2000**, *275*, 9550-9556, doi:10.1074/jbc.275.13.9550.